Chlorophyll fluorescence-based high-throughput phenotyping facilitates the genetic dissection of photosynthetic heat tolerance in African (*Oryza glaberrima*) and Asian (*Oryza sativa*) rice

Jordan K. Robson[1]*, John N. Ferguson[1,2,3]*#, Lorna McAusland[1], Jonathan A. Atkinson[1], Christine Tranchant-Dubreuil[4], Phillipe Cubry[4], François Sabot[4], Darren M. Wells[1], Adam H. Price[4], Zoe A. Wilson[1], & Erik H. Murchie[1]

[1] School of Biosciences, University of Nottingham, Sutton Bonington Campus, Loughborough, UK

[2] Department of Plant Sciences, University of Cambridge, Cambridge, UK

[3] School of Life Sciences, University of Essex, Colchester, UK

[4] Institut de Recherche pour le Developpement, 911 Av. Agropolis, 34394 Montpellier, France

[5] School of Biological Sciences, University of Aberdeen, Aberdeen, UK

* Equal contribution

\# Corresponding author; email: jfergu@essex.ac.uk

Accepted Manuscript

Downloaded from https://academic.oup.com/jxb/advance-article/doi/10.1093/jxb/erad239/7205185 by guest on 27 June 2023

© The Author(s) 2023. Published by Oxford University Press on behalf of the Society for Experimental Biology.
This is an Open Access article distributed under the terms of the Creative Commons Attribution License (https://creativecommons.org/licenses/by/4.0/), which permits unrestricted reuse, distribution, and reproduction in any medium, provided the original work is properly cited.

ORCIDs:

JKR: 0000-0002-9550-0571

JNF: 0000-0003-3603-9997

LM: 0000-0002-5908-1939

JAA: 0000-0001-7850-9876

CTD: 0000-0001-6934-1215

PC: 0000-0003-1561-8949

FS: 0000-0002-8522-7583

DW: 0000-0002-4246-4909

AHP: 0000-0003-3094-0485

ZAW: 0000-0003-0948-8770

EHM: 0000-0002-7465-845X

Highlight

A high-throughput platform for screening heat tolerance using chlorophyll fluorescence was developed and utilised to identify candidate genes underlying photosynthetic heat tolerance in African and Asian rice via GWAS.

Accepted Manuscript

Downloaded from https://academic.oup.com/jxb/advance-article/doi/10.1093/jxb/erad239/7205185 by guest on 27 June 2023

Abstract

Rising temperatures and extreme heat events threaten rice production. Half of the global population relies on rice for basic nutrition, therefore developing heat tolerant rice is essential. During vegetative development, reduced photosynthetic rates can limit growth and the capacity to store soluble carbohydrates. The photosystem II (PSII) complex is a particularly heat-labile component of photosynthesis. We have developed a high-throughput chlorophyll fluorescence-based screen for photosynthetic heat tolerance (PHT) capable of screening hundreds of plants daily. Through measuring the response of maximum PSII efficiency to increasing temperature, this platform generates data for modelling the PSII-temperature relationship in large populations in a small amount of time. Coefficients from these models (PHT traits) demonstrated high heritabilities across African (*Oryza glaberrima*) and Asian (*Oryza sativa*, Bengal Assam Aus Panel (BAAP)) rice diversity sets, highlighting valuable genetic variation accessible for breeding. Genome-wide association studies (GWAS) were performed across both species for these traits, representing the first documented attempt to characterise the genetic basis of PHT in any species to date. 133 candidate genes were highlighted. These were significantly enriched with genes whose predicted roles suggested influence on PSII activity and the response to stress. We discuss the most promising candidates for improving PHT in rice.

Keywords

chlorophyll fluorescence, photosynthesis, GWAS, heat stress, *Oryza glaberrima* (African rice), *Oryza sativa* (Asian rice)

Accepted Manuscript

Downloaded from https://academic.oup.com/jxb/advance-article/doi/10.1093/jxb/erad239/7205185 by guest on 27 June 2023

Abbreviations

ABA	Abscisic Acid
BAAP	Bengal Assam Aus Panel
F_o	Minimum fluorescence
F_m	Maximum fluorescence
F_v	Variable fluorescence
F_v/F_m	Maximum quantum yield of PSII
GO	Gene ontology
GWAS	Genome-wide association study
PHT	Photosynthetic heat tolerance
PSII	Photosystem II
SA	Salicylic acid
SNP	Single nucleotide polymorphism
QTL	Quantitative trait loci

Accepted Manuscript

Downloaded from https://academic.oup.com/jxb/advance-article/doi/10.1093/jxb/erad239/7205185 by guest on 27 June 2023

Introduction

The timing of heat stress events plays an important role in determining yield impacts for rice (Salvucci and Crafts-Brandner, 2004; Jagadish *et al.*, 2015; Zhen *et al.*, 2020; Li *et al.*, 2021). For example, high night-time temperatures increase rates of dark respiration, which in turn increase the consumption of photo-assimilates that may otherwise be translocated to reproductive sinks (Xu *et al.*, 2021). Daytime heat stress events can have substantial effects on productivity if they co-occur with anthesis (Lafarge *et al.*, 2016; Jagadish, 2020). During pre-anthesis developmental stages, heat stress events can detrimentally impact photosynthesis, which in turn impairs growth and the build-up of stem-stored water-soluble carbohydrates (WSC; Khan *et al.*, 2019; Qu *et al.*, 2021) that are important for subsequent grain filling. Therefore, the ability to limit pre-anthesis leaf senescence can be an important target trait for developing climatic resilience in rice.

The increasing frequency and intensity of heat stress events in key rice growing regions (Sun *et al.*, 2021, 2022) necessitates the development of novel heat tolerant varieties. This goal can be achieved through the identification of markers that are linked to heat tolerant loci for marker assisted breeding, or through the identification of genes that regulate natural variation in heat tolerance that can form the basis of genetic engineering. These forward genetic approaches require the capacity to link genotypic information with phenotypic information. There is an abundant supply of single nucleotide polymorphism (SNP) genotypic datasets available for rice thanks to projects such as the 3K rice genomes (Wang *et al.*, 2018). These can facilitate genome-wide association studies (GWAS) to identify genetic regions linked to traits of interest. Consequently, the bottleneck in bridging the phenotype-to-genotype gap is the ability to quickly generate high-quality phenotypic data (Araus and Cairns, 2014; Yang *et al.*, 2020; Song *et al.*, 2021). For quantifying variation in heat tolerance this is an especially troublesome barrier to progress because the infrastructure required to expose large panels or populations of rice plants to elevated temperatures is substantial. Here, prerequisites include access to large and well-regulated controlled growth facilities or the ability to leverage field trials across geographic temperature clines.

Stabilising photosynthesis under heat stress is an important determinant of heat tolerance, especially pre-anthesis, and it is phenotypically and genetically linked to the ability to stay green (Jagadish *et al.*, 2015; Ferguson *et al.*, 2020). Numerous aspects of photosynthesis are sensitive to increasing temperatures. For example, perturbed re-activation of Rubisco by rubisco activase

Accepted Manuscript

Downloaded from https://academic.oup.com/jxb/advance-article/doi/10.1093/jxb/erad239/7205185 by guest on 27 June 2023

contributes to the decline in active carbon fixation with increasing temperatures (Salvucci and Crafts-Brandner, 2004; Qu *et al.*, 2021). Moreover, as temperatures increase Rubisco specificity for carboxylation compared to oxygenation declines, therefore photorespiration increases and photosynthetic output decreases (Cavanagh *et al.*, 2022). The most heat-labile aspect of photosynthesis, however, is the photosystem II (PSII) protein complex (Yamamoto, 2016; Yoshioka-Nishimura, 2018) . PSII is the protein complex that catalyses the first reaction in photosynthesis. Here, a series of light-dependent electron-transfer reactions result in the splitting of water molecules, converting light energy into chemical energy (Shen, 2015). As temperatures increase beyond optimal, the manganese-stabilising protein of the PSII complex is released, which perturbs the oxygen evolution reaction (Thompson *et al.*, 1989; Sharkey, 2005). This damage is reversible (Lydakis-Simantiris *et al.*, 1999), however as temperatures continue to increase, PSII disassembles and there is severe denaturation of chlorophyll-containing complexes (Lípová *et al.*, 2010), representing irreparable or long term damage.

The importance of stabilised photosynthesis for facilitating heat tolerance and the integral nature of PSII to this dynamic pinpoints chlorophyll fluorescence as a technique for facilitating phenomics of heat tolerance in crop species (Ferguson *et al.*, 2021). Light energy absorbed by chlorophyll containing molecules in PSII can either facilitate photosynthesis, be re-emitted as heat, or re-emitted as light. The yield of re-emitted light (i.e., chlorophyll fluorescence) can be used to determine the quantum efficiency of PSII (Murchie and Lawson, 2013). In recent years, we and others have demonstrated that it is feasible to combine relatively low cost chlorophyll fluorescence platforms with custom methods of sample heating such as water-baths or peltier devices to screen the quantum efficiency of PSII in response to incrementally increasing temperatures across several species, e.g. rice (Ferguson *et al.*, 2020), tropical montane tree species (Feeley *et al.*, 2020), wheat (Coast *et al.*, 2022), and grapevine (Xu *et al.*, 2014). These data have been employed to determine parameters that quantify key aspects of the relationship between PSII efficiency and temperature. The most utilised of these is the critical temperature point (T_{crit}), which is the temperature point at which PSII efficiency transitions from moderate to extreme reductions, and the temperature at which point PSII efficiency is 50% of its maximum, i.e., T_{50}.

Whilst the efficiency of chlorophyll fluorescence temperature response measurements has been well demonstrated in numerous species, there have not presently been any demonstrated instances of

Accepted Manuscript
Downloaded from https://academic.oup.com/jxb/advance-article/doi/10.1093/jxb/erad239/7205185 by guest on 27 June 2023

this approach being utilised to screen broad intraspecific variation. Thus, demonstrating the applicability of this technique on a phenomics-scale is required to understand its utility for forward genetics. To this end, we set a methodological target for this study to adapt our previous approach for screening chlorophyll fluorescence temperature responses by incorporating the use of silicone heater mats to screen substantially more samples at a time. As a test case target, we sought to screen natural variation for these responses across separate African (*O. glaberrima*; Cubry *et al.*, (2018)) and Asian (*O. sativa*; Norton *et al.*, (2018)) rice diversity panels. Beyond testing the utility of our new approach for screening chlorophyll fluorescence temperature responses, we sought to (a) determine the extent to which quantitative trait loci (QTL) for photosynthetic heat tolerance (PHT, e.g., T_{crit} and T_{50}) were consistent between the two diverged rice species and (b) identify novel candidate genes for PHT as targets for developing heat tolerance in rice.

Materials & Methods

Plant material and growth conditions

Seed from all accessions comprising this study were heat treated in water at 55℃for 40 minutes to limit fungal infections and promote germination. Seeds were sown directly into 12L growth containers filled with a specialised rice compost (50:50; John Innes 3: Levington M3, The Scotts Company, Ipswich, UK). 48 plants were grown per container in a randomised design, representing a planting density of 0.05 plants cm^{-2}. 186 accessions of the Bengal Assam Asus Panel (BAAP) of *O. sativa* (Norton *et al*. 2018) and 146 accessions of *O. glaberrima* (Cubry *et al*. 2018) were grown in total (Supplemental Table S1), where the reference IR64 *O. sativa* accession was grown in each growth container.

Plants were sown and grown in a common controlled environment growth room. Here, a combination of metal halide and incandescent lamps were lowered such that the lighting intensity measured as photosynthetically active radiation (PAR) was ~550 μmol m^{-2} s^{-2} at plant level. The photoperiod was set to a 12hr day-night cycle. Temperature was set to 28℃(daytime) and 25℃ (night-time). Relative humidity (RH) stayed within a range of 50-70%.

Downloaded from https://academic.oup.com/jxb/advance-article/doi/10.1093/jxb/erad239/7205185 by guest on 27 June 2023

Accepted Manuscript

Chlorophyll fluorescence-temperature response measurements

At four-weeks post sowing, a 4-4.5cm portion of the third leaf of each plant was sampled. These leaf samples were arranged in a randomised manner on 2mm-thick damp filter paper. The damp filter paper was placed on top of a 3mm thick aluminium sheet (40cm x 60cm). Once all samples were arranged, a 1.5mm thick sheet of non-reflective glass (As described previously: Ferguson *et al.*, 2020) was placed on top of the leaf samples taking care not to disturb their positions. 100-120 samples were arranged and measured in any given *run* of measurements, where a reference map was produced on each occasion to determine the identity of each sample. Samples were collected and arranged within 45 minutes in a room directly adjacent to the controlled growth room.

The aluminium sheet containing the samples was subsequently placed on top of two adjacent 400W silicone heater mats (Model LM240, Thermosenese, Bourne End, UK) inside of a previously described (McAusland *et al.*, 2019) custom closed chlorophyll fluorescence system (PSI, Czech Republic). The temperature of both silicone heater mats was regulated by the same proportional-integral-derivative (PID) controller (Model CH102, Thermosense, Bourne End, UK). Temperature feedback to the PID controller was achieved via a K-type bead thermocouple that was placed underneath the glass sheet adjacent to leaf samples, therefore the PID controller regulated the temperature of the heater mats according to the temperature adjacent to samples on top of the filter paper. Through testing with a separate thermocouple, we determined that as long as the thermocouple regulating the PID controller was between the glass sheet and the filter paper, its specific position did not influence the temperature of ten random points across the entire temperature-regulated area containing the samples. Further testing demonstrated the temperature at the position of the regulating thermocouple never overshot, regardless of the temperature set point.

Before measurements of chlorophyll fluorescence, samples were allowed to dark adapt for 45 minutes. After this point, a measuring light pulse was switched on to provide a measure of minimal chlorophyll fluorescence (F_o). A follow-up saturating light pulse was used to provide a measure of maximum chlorophyll fluorescence (F_m). Variable fluorescence (F_v) was calculated as F_m-F_o and the maximum quantum efficiency of PSII was calculated as F_v/F_m. Following this room temperature measurement of F_v/F_m, the PID controller was switched on at an initial temperature of 25°C Once the set temperature was reached a timer was set for two minutes. After this two-minute period, the aforementioned chlorophyll fluorescence measurements were performed again. This was repeated

Downloaded from https://academic.oup.com/jxb/advance-article/doi/10.1093/jxb/erad239/7205185 by guest on 27 June 2023

Accepted Manuscript

at each incremental 1°C of temperature up to 55°C, such that we obtained a value for F_v/F_m at 30 temperature points and room temperature (Supplemental Video 1).

On each day of measurements, we performed one round of measurements starting with sample preparation at 0900, which was typically completed around 1100. A second round of measurements was then performed starting with sample preparation at 1130, which was typically completed at around 1330.

Estimation of T_{crit}, T_{50}, m_1, and m_2

Raw data coming from the FluorCam 7 software used to operate the closed chlorophyll fluorescence system was quality checked and formatted within R as described previously (Ferguson *et al.*, 2020) utilising the following packages: plyr (Wickham, 2011), reshape2 (Wickham, 2007), and ggplot2 (Wickham, 2009).

We estimated T_{crit}, m_1, and m_2 via the breakpoint modelling approach we have described previously (Ferguson *et al.*, 2020) that utilises the segmented() function in the R package segmented (Muggeo, 2017). T_{crit} is a computationally determined breakpoint in the relationship between F_v/F_m and temperature where the response of F_v/F_m transitions from a slow to a rapid decline. m_1 and m_2 are the slope values from linear models that define F_v/F_m as a function of temperature before and after T_{crit} (Supplemental Fig. S1). Additionally, for this study we also estimated T_{50}, which we define as the temperature point where F_v/F_m is 50% of the maximum value estimated on a sample-by-sample basis. This was achieved first by extracting the F_v/F_m value measured at 25°C, which was always the maximum value for F_v/F_m. We then constructed an inverse linear model of that used to estimate T_{crit}, i.e., where temperature becomes the dependent variable and F_v/F_m is the independent variable. We then generated a segmented model based on this linear model as described previously. Using this segmented model, we predicted the temperature (*y*), where F_v/F_m (*x*) was 50% of the previously extracted maximum value.

Accepted Manuscript

Downloaded from https://academic.oup.com/jxb/advance-article/doi/10.1093/jxb/erad239/7205185 by guest on 27 June 2023

Statistical analyses

To account for unwanted variance with the traits of interest, we performed linear mixed models to extract genotype variance components using the lmer() function from the lme4 R package (Bates *et al.*, 2015). The models were constructed as:

$$Y = Z_{ij} + Z_k + Z_l + e$$

Here, Y represents the vector of responses (either T_{crit}, T_{50}, m_1, or m_2); Z represent a matrix of random effects due to the interaction between round and time of measurements, ij, the container from which a plant originated, k, and the genotype, l; and e is vector of random errors. Genotype Best Linear Unbiased Predictors (BLUPs) were extracted from these models using the ranef() function from lme4. BLUPs were added to the population mean for each trait obtained from the above-described models to generate adjusted means that thereby controlled for unexplained variance in the traits. This approach was taken for each species separately since the experiments for each were also performed separately. Unless stated otherwise, all further statistical analyses and genetic mapping were performed using BLUPs (Supplemental Table S2). The variances extracted from each linear mixed model were used to estimate broad sense heritability (H^2) as the ratio of the variance due to genotype, i.e., genotypic variation, and the summation of variation from all sources, i.e., phenotypic variance.

For each species, we explored correlations between all pairwise trait interactions via Pearson's correlations coefficients. These interactions were visualised via a network plot constructed using the corr R package. Further graphical plotting was performed using the ggplot2 R package, with some post processing performed in Affinity Designer (Serif; www.serif.com).

Genome Wide Association Mapping

Since genotypic data was separate for the two species, Genome Wide Association Studies (GWAS) were carried out individually for each population using previously published pipelines. All SNP marker sets used in this study were aligned to the Nipponbare high quality reference genome (IRGSP-1.0), with bioinformatic pipelines, software and SNP filtering steps all described in more detail in Norton *et al.* (2018) and Cubry *et al.* (2018). For the *O. sativa* Bengal Assam Aus Panel (BAAP), GWAS was undertaken using PIQUE (Parallel Identification of QTLs Using EMMAX) as in Norton *et al.* (2018) and LFMM was subsequently performed using the lfmm R package (Caye *et al.*, 2019), using the published 2,053,863 imputed SNP marker-set filtered for MAF > 0.05 and missing

Accepted Manuscript

Downloaded from https://academic.oup.com/jxb/advance-article/doi/10.1093/jxb/erad239/7205185 by guest on 27 June 2023

data < 0.1 (Norton *et al.*, 2018). GWAS of the *O. glaberrima* population was performed via a bioinformatics pipeline utilising GAPIT (Lipka *et al.*, 2012) and encompassing multiple models including LFMM and EMMA, as in Cubry *et al.* (2020), using 892,539 imputed SNP markers (Cubry *et al.*, 2018) filtered for minor allele frequency (MAF) > 0.05 and missing data < 0.05. Results from all analyses were visualised via QQ- and Manhattan plots using the qqman R package (Turner, 2018). QQ-plots were used to assess the two best fitting GWAS models for each trait within each population and to determine the significance threshold for SNP calling within these models. For most traits, visualising the distribution of the GWAS p-values (Supplemental Fig. S2-S6) demonstrated a reduction in their effect compared to what would be expected of a normal distribution, likely due to the high polygenic nature of photosynthetic heat tolerance. Therefore, we used a less stringent threshold of -log10(p-value) < 4 to determine SNPs of interest in most models.

A linkage disequilibrium (LD)-based clumping procedure on PLINK (Purcell *et al.*, 2007) was used to process significant SNPs into putative QTLs based on average genome-wide LD (150kb and 243kb respectively in *O. glaberrima* and BAAP populations, in accordance with previously published data). To reduce the likelihood of highlighting false positives, QTLs were discarded if they contained less than 2 SNPs (Norton *et al.*, 2018).

Local LD was calculated between each SNP pair within a 500kb region either side of each QTL peak for the BAAP population using the LDheatmap R package (Shin *et al.*, 2006) to create LD heatmaps and matrices. All genes within these 1Mb regions were annotated using the IRGSP-1.0 (International Rice Genome Sequencing Project) reference genome assembly from the Rice Annotation Project Database (RAP-DB). Genes containing at least one SNP in LD (r^2>0.3) with a significant SNP from GWAS were extracted for further analysis. This list of genes were used for gene ontology (GO) enrichment analyses using the PANTHER classification system (Mi *et al.*, 2019). Candidate genes were shortlisted based on functional classification, GO, homology, expression over developmental stages based on information from the Rice Genome Annotation Project (RGAP), RAP-DB & RiceXPro and differential expression within published rice heat stress transcriptomic studies (Liu *et al.*, 2020; Sharma *et al.*, 2021).

Accepted Manuscript

Downloaded from https://academic.oup.com/jxb/advance-article/doi/10.1093/jxb/erad239/7205185 by guest on 27 June 2023

Results

Analysis of phenotypic variation

Our data acquisition and processing pipeline facilitated the generation of a dataset comprising the photosynthetic heat tolerances (PHTs) of 146 *O. glaberrima* and 186 *O. sativa* accessions within five weeks of sowing seeds (Fig. 1; Supplemental Table S1). Through segmented modelling, we benchmarked PHT as T_{crit}, T_{50}, m_1, and m_2 as described previously (Ferguson *et al.*, 2020; Supplemental Fig. S1), thereby characterising the whole response of F_v/F_m to rapidly increasing temperatures (Fig. 2).

In general, the intraspecific variation for PHT within *O. sativa* was greater than the intraspecific variation within *O. glaberrima* (Fig. 3). For example, m_2 varied from 0.142-0.169 in *O. glaberrima* (Fig. 3C) and from 0.092-0.206 in *O. sativa* (Fig. 3D). Similarly, T_{crit} varied from 45.7-48.8 in *O. glaberrima* (Fig. 3E) and from 47.3-50.7 in *O. sativa* (Fig. 3F).

The variation in PHT within *O. sativa* was shifted towards reduced sensitivity to temperature compared to *O. glaberrima*. For example, the population means for the slope metrics (m_1 and m_2), were greater in *O. glaberrima* (0.0053 and 0.151 respectively) compared to *O. sativa* (0.0049 and 0.132 respectively; Fig. 3A-D), where reduced values here indicate a less extreme response. Similarly, the range in T_{crit} and T_{50} values and their associated population means were reduced in *O. glaberrima* (44.7 and 46.8) compared to *O. sativa* (46.4 and 48.8; Fig. 3E-H), where greater values here indicate a less sensitive response to temperature, i.e., F_v/F_m reaches the critical temperature point and 50% of the maximum F_v/F_m at a higher temperature in general in *O. sativa*.

Except for the m_2 parameter estimated in *O. glaberrima*, for which our mixed effect model did not well explain the data (R^2 = 0.18), all of the PHT metrics estimated across both species demonstrated moderate-to-high broad sense heritabilities considering their complex nature (H^2; Table 1). With the most heritable trait being T_{crit}, which was estimated at 0.65 in *O. sativa* and 0.61 in *O. glaberrima*. The least heritable trait for *O. glaberrima* was m_2 (0.09), which conversely had a moderate heritability of 0.53 in *O. sativa*. The least heritable trait for *O. sativa* was m_1 (0.48), which was also much less heritable in *O. glaberrima* (0.27).

The only common correlation for both species was the strong positive correlation between T_{crit} and T_{50}, suggesting that genotypes that transition to the m_2 phase of the association between temperature and F_v/F_m fastest reach 50% of maximum F_v/F_m at the lowest temperatures, i.e.,

Downloaded from https://academic.oup.com/jxb/advance-article/doi/10.1093/jxb/erad239/7205185 by guest on 27 June 2023
Accepted Manuscript

reduced PHT (Supplemental Table S3). The correlation between the T_{crit} parameter and the m_2 parameter was significant for both species, however the direction of the correlation was reversed. Here, these parameters shared a positive correlation across the *O. sativa* accessions, but negative across the *O. glaberrima* accessions. This suggests that *O. sativa* accessions that transition to the m_2 phase at the lowest temperature demonstrate the lowest rate of decline in F_v/F_m from that point onward, where it suggests the opposite for the *O. glaberrima* accessions.

For *O. glaberrima* the only additionally significant correlation was the positive correlation between m_1 and T_{50}, suggesting that *O. glaberrima* accessions with the fastest initial decline in F_v/F_m reach 50% of the maximum F_v/F_m at the lowest temperature. This is also reflected in m_1 and T_{crit} showing a marginally non-significant (p-value = 0.06) positive correlation also (Supplemental Table S3). For *O. sativa,* significant positive correlations were detected between T_{crit} and m_1 and between m_1 and m_2 (Supplemental Table S3), which suggests that lines that respond most strongly to the initial temperature increases: a) transition to the m_2 phase quickest; and b) that they also have the fastest rates of decline in F_v/F_m after the transition. Finally, m_2 and T_{50} demonstrated a significant negative correlation across the *O. sativa* accessions (Supplemental Table S3), which suggests that lines which have the fastest rate of decline following the T_{crit} point reach 50% of maximum F_v/F_m at the lowest temperatures.

Genome-wide association mapping

The T_{50} and T_{crit} parameters demonstrated the highest heritabilities across the two species and were phenotypically linked to m_1 and m_2 in the majority (Table 1; Supplemental Table S3), consequently we focused on these traits for our GWAS.

Marker-trait associations were tested using at least two different models: efficient mixed model analysis (EMMA, (Kang *et al.*, 2008)) and a latent factor mixed model (LFMM, (Frichot *et al.*, 2013)), with additional computation of other GAPIT models including FarmCPU in the *O. glaberrima* population. For each trait within the two populations, we determined the best-fit model based on observations of the QQ-plots, which describe the distribution of the p-values associated with all SNPs against what would be expected of a normal distribution (Supplemental Fig. S2-5). Within the *O. sativa* population there was little difference between the QQ-plots, therefore EMMA was used as the best-fit for both T_{50} and T_{crit}, whereas in *O. glaberrima* LFMM was superior for T_{50} whilst FarmCPU fit T_{crit} marginally better than EMMA. QQ-plots were further used to determine a cut-off significance threshold for SNPs. These plots suggested that T_{50} and T_{crit} were polygenic in both species (Supplemental Fig. S2-S5) and that a stringent significance threshold would be inappropriate

Downloaded from https://academic.oup.com/jxb/advance-article/doi/10.1093/jxb/erad239/7205185 by guest on 27 June 2023

Accepted Manuscript

for identifying SNPs of interest. Thus, to identify QTLs we employed a threshold of $-\log_{10}(p) > 4$ in all but one of the models (T50-Glab-LFMM; Supplemental Table S4).

Significant SNPs were clumped into putative QTLs containing two or more significant SNPs based on global linkage disequilibrium (LD) of 150kb in *O. glaberrima* (Cubry *et al.*, 2018) and 243kb within the *O. sativa* BAAP population (Norton *et al.*, 2018). Through comparison of the best-fitting GWAS models, 15 distinct QTLs were identified within the *O. sativa* and *O. glaberrima* populations (Table 2, Fig. 4), with high consensus in SNPs within these regions between the two best-fitting models for each trait. Whilst there were no overlapping QTL regions between the two species, there was overlap between traits within the *O. sativa* population. For example, within both of the T_{50} QTLs on chromosome 2 (Os-T50-2a and Os-T50-2b), and within Os-T50-11a, a singular significant SNP was also identified for T_{crit}. Likewise, a significant T_{50} association was highlighted in Os-Tcrit-11a (Fig. 4).

Whilst most of the QTLs identified from this PHT screen appear to be novel there are a couple that overlap with previously identified heat-tolerance QTLs. The BAAP population-specific T_{crit} QTLs on chromosome 3 (Os-Tcrit-3) and chromosome 5 (Os-Tcrit-5) overlap respectively with slpc3.1, shoot length under heat stress (Kilasi *et al.*, 2018) , and qhts-5, spikelet fertility under heat (Ishimaru *et al.*, 2016). Also of note with respect to *O. glaberrima*, is the T_{50} QTL on chromosome 8 (Og-T50-8) which is just 236kb from a QTL identified in environmental GWAS by Cubry *et al.* (2020) for BIOCLIMATIC PRINCIPLE COMPONENT 2, which is explained primarily by the mean temperatures of the driest and coldest quarters. As the *O. glaberrima* SNP dataset was generated using alignment to the *O. sativa* Nipponbare reference genome (Cubry *et al.*, 2018) the region between the two QTLs was investigated using the NCBI database. This identified 31 genetic loci, 14 of which have orthologues in *O. glaberrima* (Supplemental Table S5). These genes include those with roles in heat tolerance (Os08g0135900) and ROS homeostasis (Os08g0133000 and Os08g0133700) as we discuss later.

Since the genome is better annotated for *Oryza sativa*, and the BAAP population has been selected specifically for its increased abiotic stress resources, we performed a more detailed downstream bioinformatics analysis of all the QTLs identified within the BAAP population. Local linkage disequilibrium (LD) around each QTL was calculated to identify genes co-localising with the significant SNPs (Fig. 5). This approach identified 133 genes within LD (r^2>0.3) of significant SNPs (Supplemental Table S6). We performed Gene Ontology (GO) enrichment analyses to benchmark the likelihood of these genes being involved in PHT. Here, we tested whether these 133 genes were significantly enriched for GO terms associated with biological processes, molecular functions, and cellular components. No GO cellular component terms were identified as significantly enriched in this set of genes, but terms for biological processes and molecular processes were enriched

Accepted Manuscript

Downloaded from https://academic.oup.com/jxb/advance-article/doi/10.1093/jxb/erad239/7205185 by guest on 27 June 2023

compared to what would be expected according to how many genes within the rice genome represent those terms (Fig. 6, Supplemental Table S7). For biological processes, five granular (specific) terms were enriched: "regulation of salicylic acid biosynthetic processes", "peptidyl-tyrosine phosphorylation", "cell surface receptor signalling pathway", "defense response", and "response to other organism" (Fig. 6A). Five granular terms were also enriched for molecular functions: "transmembrane receptor protein kinase activity", "calmodulin binding", "ADP binding", "protein serine/threonine kinase activity'', and "ATP binding" (Fig. 6B).

To pinpoint loci which might underlie photosynthetic heat tolerance we analysed the functional annotation, GO terms and literature associated with each of these genes alongside available RNASeq data showing transcriptomic changes in response to heat. We found that 19 of these genes are differentially expressed in response to heat in either IR64 or Annapurna seedlings according to previously published RNASeq analysis (Sharma *et al.*, 2021) and 11 genes are expressed in the chloroplast according to GO annotation of cellular compartment (Supplemental Table S6). 11 of the genes, or their homologs, reportedly have a function in stress response, photosynthesis or carbon partitioning, chloroplast development, stomatal density or senescence according to a literature search. Taken together, this generated a shortlist of 30 genes (Table 3) that are strong candidates for the QTLs identified within this study.

Discussion

Heritable variation in photosynthetic heat tolerance highlights the development of a new breeding tool

Performing large-scale screening of heat tolerance in any crop is hampered by numerous logistical issues relating to space to grow plants and infrastructure to elevate temperatures both in controlled and field environments (Sharma *et al.*, 2017; Ruiz-Vera *et al.*, 2018). Consequently, there is a strong requirement to develop platforms that bypass these hurdles and facilitate the rapid generation of data relating to heat tolerance. Chlorophyll fluorescence techniques are rapid and can provide information on the efficiency of particularly heat-labile components of photosynthesis that are important for defining growth and productivity (Maxwell and Johnson, 2000; Murchie and Lawson, 2013). Furthermore, it has been demonstrated that measuring various different aspects of photosynthesis on excised leaves via chlorophyll fluorescence is strongly representative of measuring the same parameter on leaves still attached to the plant in numerous crop species

Accepted Manuscript

Downloaded from https://academic.oup.com/jxb/advance-article/doi/10.1093/jxb/erad239/7205185 by guest on 27 June 2023

(McAusland *et al.*, 2019; Ferguson *et al.*, 2023). This therefore opens up the opportunity to utilise chlorophyll fluorescence as a platform for rapidly screening heat tolerance. In our previous work, we have shown that T_{crit} and m_1 as measured on excised leaf segments from rice seedlings is able to forecast adult vegetative heat tolerance measured as stay green (Ferguson *et al.*, 2020), which is a common breeding-based method of scoring abiotic stress tolerance (Jagadish *et al.*, 2015). Although effective, this previous approach suffered from throughput limitations. With this present study, these limitations were resolved by developing a heating system using silicone heater mats instead of relying on a water bath system.

Using this system, we detected significant genetic variation for PHT metrics (Fig. 3). Moreover, the broad sense heritability of these metrics were high (Table 1), especially compared to studies that have measured similar chlorophyll fluorescence parameters across diversity in other species, where heritabilities tend to be much lower (Čepl *et al.*, 2016; Herritt *et al.*, 2018; Burgess *et al.*, 2020; Herritt and Fritschi, 2020). Indeed the heritabilities we observed are much more similar to those observed in a precisely controlled phenomics platform designed for measuring chlorophyll fluorescence in Arabidopsis (Flood *et al.*, 2016). This suggests that our phenotyping platform limits environmental noise that may confound our measurements and highlights the existence of genetic mechanisms underlying the observed variation in both species. These are attractive features of a phenotyping platform and suggest that it could provide cost-free, repeatable and potentially valuable data to use as covariates in selection models for rice breeding. Breeding for yield while also considering information relating to heat tolerance has the potential to enhance the climatic resilience of future, highly productive rice varieties.

The main coefficients obtained from the segmented modelling used to characterise the F_v/F_m temperature response, i.e., T_{crit} and T_{50} (Fig. 2), demonstrated strong positive correlations (Supplemental Table S3). However, the correlations were not perfect (Supplemental Table S3; R^2 = 0.73 and 0.65 in *O. glaberrima* and *O. sativa* respectively). Therefore, the aspect(s) of the response of PSII to incrementally increasing temperatures that they are characterising are different. This is valuable for gene identification, because it allows us to detect unique QTL underlying the different traits, even though they are positively correlated. This is evidenced by our results, for example mapping for T_{crit} and T_{50} can pick up colocalising QTL (e.g., on chromosome 2 and 11 in *O. sativa*; Fig.

Downloaded from https://academic.oup.com/jxb/advance-article/doi/10.1093/jxb/erad239/7205185 by guest on 27 June 2023
Accepted Manuscript

4-5), but occasionally genetic regions only appear important for regulating one of these traits within a species (e.g., on chromosome 8 and 11 in *O. glaberrima*; Fig. 4).

In general, our data suggest that our Assam Aus diversity set of *O. sativa* is more heat tolerant than the surveyed *O. glaberrima* lines (Fig. 3). It is also interesting to note the differences in correlations between PHT parameters across the species. We have previously discussed in detail what these parameters reflect in terms of PSII activity and its response to heat stress (Ferguson *et al.*, 2020). Here, we note in particular that T_{crit} and m_2 are positively correlated in *O. sativa* but negatively correlated in *O. glaberrima* (Supplemental Table S2). m_2 describes the relationship between F_v/F_m and temperature after the point (T_{crit}) where its transitions to a rapid decline and refers more to heat *resistance* than *tolerance* in that it gauges the capacity to restrain permanent damage as opposed to maintaining typical plant function, *i.e., tolerating* high temperatures (Thompson *et al.*, 1989; Zhang and Sharkey, 2009; Ferguson *et al.*, 2020). The negative correlation between T_{crit} and m_2 in *O. glaberrima* appears initially more logical since it suggests that lines that transition to the m_2 phase faster, i.e., have reduced T_{crit}, have a faster rate of PSII disassembly as well. This is indicative of *O. glaberrima* genotypes with high heat tolerance also having high heat resistance (reduced rate of decline of F_v/F_m in the secondary temperature range after T_{crit}).The positive correlation between these parameters in *O. sativa* would suggest the opposite. This highlights uncoupling in *O. sativa* between the tolerance of PSII to heat, which is likely conferred through mechanisms related to the capacity of the thylakoid membranes to unfold for PSII repair (Theis and Schroda, 2016), and its resistance to heat after the transition to the point where PSII deconstruction begins to take place. The underlying mechanisms that confer potential trade-offs here are of interest and could help guide target traits for crop improvement depending on the environment being selected for, e.g., mild or extreme heat stress.

GWAS for PHT identifies genes enriched with predicted functions associated with regulating PSII activity

Through GWAS, we have identified novel and distinct QTLs underlying PHT in diverse rice populations (Fig. 4-5, Table 2). Three times as many T_{crit} and T_{50} QTL were identified for *O. sativa* than for *O. glaberrima*. This reflects our observation that heritability for all PHT traits was higher in *O. sativa* than in *O. glaberrima* (Table 1) and that *O. sativa* was in general more tolerant to heat stress, with higher population means for T_{crit} and T_{50} (Fig. 3). Taken together, these findings suggest that

Accepted Manuscript
Downloaded from https://academic.oup.com/jxb/advance-article/doi/10.1093/jxb/erad239/7205185 by guest on 27 June 2023

selection strength for PHT may have been reduced in *O. glaberrima* or that it harbours fewer, but stronger effect PHT-associated genes compared to the Asian species. Compared to other types of *O. sativa*, the *aus* varieties are considered to be highly stress tolerant. This may be a consequence of *aus* cultivars originating predominantly from Bangladesh and India (Ali *et al.*, 2011) since there appears to have been strong selective pressure on rice cultivated in the stress-prone Bangladesh and adjacent regions to be more resilient to environmental stresses (Bin Rahman and Zhang, 2018). This increased PHT is unlikely to be representative of the *O. sativa* species as a whole. The *O. glaberrima* accessions were selected from ranges of temperature, rainfall, and altitudes across Western Africa, but it is unclear how limited the variation in this region might be compared with that across Asia (Cowling *et al*. 2021). Regardless, it seems that PHT mechanisms are divergent between the two populations sampled as we found no overlapping QTLs.

The enriched GO terms within the candidate genes highlight the utility of our phenotyping and GWAS approach. The biological processes and molecular functions associated with these terms pinpoint roles for these genes in PSII activity and the response to stress (Fig. 6). The role of PSII in the non-cyclic photophosphorylation conversion of ATP from ADP (Arnon, 1984) is reflected in the enrichment of genes associated with the "ADP binding" molecular function GO term. Additionally, the enriched GO terms associated with tyrosine activity (i.e., "peptidyl-tyrosine phosphorylation" and "transmembrane receptor protein tyrosine kinase activity") further highlight a role in PSII activity for many of the candidate genes, as tyrosine phosphorylation involves the transfer of a phosphate away from ATP (Mühlenbeck *et al.*, 2021), which may in turn increase the demand for ATP, thereby influencing PSII activity. Indeed, the increasing demand for ATP may be a result of the heat shock damage to PSII, since ATP is demonstrated to be the driving force in the repair of PSII during photoinhibition (Murata and Nishiyama, 2018). Here, ATP-dependent regulation of PSII repair under environmental stress is associated with synthesis of the D1 protein, which is the primary target of PSII photooxidative damage (Yoshioka and Yamamoto, 2011). A further enriched GO term of interest that highlights the efficiency of our GWAS in identifying genes involved in PSII activity is the 'calmodulin binding' molecular function (Fig. 6B). Calcium is an essential cofactor for the oxygen evolving complex of PSII that catalyses the oxidation of water (Barry *et al.*, 2005; Wang *et al.*, 2019), thus it is logical that predicted calmodulins (calcium-binding proteins) may be enriched in our candidate genes. Further support is lended to this end from studies that have demonstrated that exogenous application of Ca^{2+} can stabilise PSII activity under heat stress (Tiwari *et al.*, 2019; Zheng *et al.*, 2022), thereby highlighting the importance of Ca^{2+} homeostasis for PHT, potentially achieved through calmodulin-mediated Ca^{2+} signalling.

Accepted Manuscript

Downloaded from https://academic.oup.com/jxb/advance-article/doi/10.1093/jxb/erad239/7205185 by guest on 27 June 2023

Across the 133 candidate genes, the GO term most enriched was that associated with salicylic acid (SA) biosynthesis (Fig. 6A). SA has been well demonstrated to play a role in influencing the response of plants to heat stress, where it is best characterised by inducing antioxidant activity (Dat *et al.*, 1998; Nazar *et al.*, 2011; Khan *et al.*, 2013; Jahan *et al.*, 2019; Janda *et al.*, 2020). Antioxidant enzymes can protect PSII from damage due to reactive oxygen species (ROS; Das and Roychoudhury, (2014)). There is evidence suggesting that during rapid stress events, SA accumulation can have an alleviating effect on PSII photoinhibition. For example, Chen *et al.* (2020) demonstrated that under high light stress, SA accumulation increased photoprotection in *Arabidopsis thaliana* (Arabidopsis) by enhancing the phosphorylation of the D1 and D2 PSII proteins and by reducing the rate of disassembly of the PSII-LHCII super complexes. The same authors have also shown that SA has a similar photoprotective role in wheat seedlings (Chen *et al.*, 2016).

Additionally enriched GO terms highlight the potential role of genes with defense roles regulating variation in T_{crit} and T_{50} (Fig. 6A). PSII is important for plant immunity because of its role in producing ROS, which can be important retrograde signalling molecules for coordinating defense responses (Järvi *et al.*, 2016, Foyer & Hanke, 2022). Consequently, genes involved in regulating ROS production to protect PSII during heat stress may additionally have roles in the signalling pathways associated with plant immunity. Indeed, disrupting chloroplastic function has been shown to impair resistance in wheat to *Septoria* leaf blotch (Lee *et al.*, 2015), where resistance to this end is associated with photoprotection (Ajigboye *et al.*, 2021).

We have confidence in our GO enrichment approach for validating our GWAS because of the identified and discussed terms. Additionally, we believe it is a valid approach in this instance because of the number of QTL identified. Since we identified more than 10 QTL for T_{crit} and T_{50} and inputted associated genes into the GO enrichment analyses we would expect some enrichment in genes involved in PSII activity. This would not be the case if we had identified only a few (~1-5 QTL). Indeed, the number of genes associated with the enriched terms is small and consistent with the number of identified QTL, but the fold enrichment and the significance attached to them is high (Fig. 6).

Promising candidate genes for the development of heat tolerance in rice

Our approach for narrowing down the candidate genes (Fig. 1, Materials and methods) identified 30 genes for which we have high confidence in their role in PSII activity and/or heat tolerance (Table 3), we highlight the most promising of these below.

Downloaded from https://academic.oup.com/jxb/advance-article/doi/10.1093/jxb/erad239/7205185 by guest on 27 June 2023

Accepted Manuscript

We identified two genes whose Arabidopsis homologs are known to play essential roles in chloroplast development (Table 3), namely DELAYED GREENING 1 (DG1) and ALBINO OR PALE GREEN 3 (APG3). Knockout mutants of these two genes exhibit striking phenotypes. *dg1* mutant seedlings exhibit initially pale young leaves which gradually green to WT levels (Chi *et al.*, 2008) whilst *apg3* mutants lack chlorophyll pigments and cannot photosynthesise (Motohashi *et al.*, 2007). Both genes appear to be involved in the formation of thylakoid membranes. The location of PSII within the thylakoid membrane further highlights the role these genes likely play in the activity of PSII where stable thylakoid complex assembly and maintenance will play an important role in heat tolerance. Furthermore, OsDG1 exhibits a 2-fold increase in expression in response to 42°C heat stress in IR64 seedlings (Sharma *et al.*, 2021). Mutations in AtDG1 have also been shown to result in temperature sensitivity and reduced F_v/F_m at high temperatures relative to wildtype, where the same phenotype is not observed under optimal growing temperatures (Sun *et al.*, 2020), here DG1 appears to be important for regulating chloroplastic mRNA editing at elevated temperatures.

We additionally identified several other genes with demonstrable roles in photosynthesis (Table 3). For example, GOLGI LOCALIZED MONOSACCHRIDE TRANSPORTER 1 (GST1) has been shown to play a role in sugar accumulation during abiotic stress (Cao *et al.*, 2011) and its Arabidopsis homolog, pGlct, is involved in carbon partitioning, with mutants showing decreased photosynthesis (Cho *et al.*, 2011). pGlct has also been demonstrated to have a role in sugar (maltose) accumulation for conferring photoprotection of PSII (Kaplan and Guy, 2005). A further identified photosynthesis-related gene of interest is SPOTTED LESSION 40 (SPL40, Table 3). SPL40 appears to be critical in activating SA signalling pathways and *spl40* mutants show hypersensitivity to light and a compromise in ROS homeostasis. This is associated with a downregulation in the expression of photosynthesis-associated genes and a reduction in chlorophyll content (Sathe *et al.*, 2019).

The Calmodulin-Like Protein Gene 21 (CML21) was identified within the Os-Tcrit-5 QTL. In Arabidopsis, CML21 functions as a calcium sensor coordinating Ca^{2+} signalling (McCormack and Braam, 2003), highlighting a potential role in Ca^{2+} homeostasis for protecting PSII. Further to this, the study of (Aleynova *et al.*, 2020) showed in grapevine that the native CML21 is differentially expressed in response to high temperatures. They also showed that heterologous overexpression of grapevine CML21 in Arabidopsis disrupted biomass accumulation in response to heat stress, highlighting the importance of functional CML21 activity.

Also associated with the Os-Tcrit-5 QTL, were genes with sequence similarity to the Arabidopsis plasma-membrane localized receptor-like kinase FERONIA gene (Table 3, Supplemental Table S6). Recent evidence has pinpointed FERONIA in having a key role in regulating tolerance to

Accepted Manuscript

Downloaded from https://academic.oup.com/jxb/advance-article/doi/10.1093/jxb/erad239/7205185 by guest on 27 June 2023

photooxidative stress (Wang *et al.*, 2020*b*; Shin *et al.*, 2021; Jing *et al.*, 2022). For example, Arabidopsis *fer* mutants are hugely light sensitive and demonstrate leaf bleaching when exposed to just moderate light intensities (Shin *et al.*, 2021). Here, *fer* mutants do not appear to be able to induce expression of key stress genes in response to light, such that ROS over-accumulate causing severe damage to PSII. In apple, overexpression of a native FERONIA gene markedly improved drought tolerance (Jing *et al.*, 2022). Here, FERONIA overexpression lines demonstrated significantly reduced photosystem damage and improved rates of photosynthesis compared to wildtype apple after seven days of water withdrawal. The findings of these studies highlight the potential role of our identified FERONIA genes for improving photoprotection in response to heat in rice.

The recent study by Cubry *et al.* (2020) included the results of environmental-GWAS in *O. glaberrima*, where the authors performed GWAS on bioclimatic parameters specific to the point of origin of the same *O. glaberrima* accessions used in this present study. These bioclimatic parameters include those related to temperature. Since we are measuring temperature responses, we might expect to observe some overlap between environmental QTL detected by Cubry *et al.* (2020) and our QTLs. To this end, we observed the colocalization (within 250kb) of our Og-T50-8 QTL and a QTL detected for mean temperature-related parameters; 31 genes lie within this region (Supplemental Table S4) and include those with potential roles in conferring heat tolerance (Table 3). Os08g0135900, for example, is orthologous to Arabidopsis TRYPTOPHAN SYNTHASE B SUBUNIT 1 (TSB1), and has been shown to modulate tryptophan and abscisic acid (ABA) biosynthesis to coordinate stress responses and growth in Arabidopsis (Liu *et al.*, 2022) and rice (Dharmawardhana *et al.*, 2013). Additionally, two genes in this region (Os08g0133000 and Os08g0133700) encode plant cysteine oxidases (Table 3, Supplemental Table S4). These enzymes are crucial in oxygen sensing and triggering various plant stress responses through the N-degron pathway to maintain cellular homeostasis in response to intracellular O_2 and ROS accumulation (Holdsworth *et al.*, 2020; Heo *et al.*, 2021).

Conclusion

With this study, we have adjusted our previous approach to measure the response of the maximum efficiency of PSII to increasing temperatures, such that it now truly represents a phenomics-like platform. The high estimates of heritability and broad genetic variation characterised through this platform highlights its utility for crop breeding, where T_{crit} and T_{50} could represent important covariates in rice selection models. Finally, we have assembled a list of high-confidence candidate genes representing targets for improving heat tolerance in rice.

Downloaded from https://academic.oup.com/jxb/advance-article/doi/10.1093/jxb/erad239/7205185 by guest on 27 June 2023

Accepted Manuscript

Contributions

All authors contributed to the design of the study. JNF performed the experiments. JR performed the GWAS. LM proposed the screening method and aided with the development. JAA and DMW put together the silicone heater mat setup. AP provided the *O. sativa* germplasm and genetic data. CTD, PC, and FS provided the *O. glaberrima* germplasm and genetic data. JR and JNF performed additional data analyses. JR and JNF wrote the manuscript with input from all authors.

Acknowledgements

We are grateful to the University of Nottingham glasshouse staff for their assistance with general plant maintenance. We acknowledge the insight of two anonymous reviews whose comments greatly improved this manuscript.

Conflict of Interest

The authors declare no conflicts of interest.

Funding Statement

JR and JNF were supported by the Palaeobenchmarking Resilient Agriculture Systems (PalaeoRAS) project funded by the Future Food Beacon of the University of Nottingham.

Data Availability Statement

All data presented in this paper are available in the supplemental material.

Accepted Manuscript

Downloaded from https://academic.oup.com/jxb/advance-article/doi/10.1093/jxb/erad239/7205185 by guest on 27 June 2023

References

Ajigboye OO, Jayaweera DP, Angelopoulou D, Ruban AV, Murchie EH, Pastor V, Summers R, Ray RV. 2021. The role of photoprotection in defence of two wheat genotypes against *Zymoseptoria tritici*. Plant Pathology **70**, 1421–1435.

Aleynova OA, Kiselev KV, Ogneva ZV, Dubrovina AS. 2020. The Grapevine Calmodulin-Like Protein Gene Is Regulated by Alternative Splicing and Involved in Abiotic Stress Response. International journal of molecular sciences **21**.

Ali ML, Liakat Ali M, McClung AM, Jia MH, Kimball JA, McCouch SR, Eizenga GC. 2011. A Rice Diversity Panel Evaluated for Genetic and Agro-Morphological Diversity between Subpopulations and its Geographic Distribution. Crop Science **51**, 2021–2035.

Araus JL, Cairns JE. 2014. Field high-throughput phenotyping: the new crop breeding frontier. Trends in Plant Science **19**, 52–61.

Arnon DI. 1984. The discovery of photosynthetic phosphorylation. Trends in Biochemical Sciences **9**, 258–262.

Barry BA, Hicks C, De Riso A, Jenson DL. 2005. Calcium ligation in photosystem II under inhibiting conditions. Biophysical journal **89**, 393–401.

Bates D, Mächler M, Bolker B, Walker S. 2015. Fitting Linear Mixed-Effects Models Using**lme4**. Journal of Statistical Software **67**.

Bin Rahman ANMR, Zhang J. 2018. Preferential Geographic Distribution Pattern of Abiotic Stress Tolerant Rice. Rice **11**, 10.

Burgess SJ, de Becker E, Cullum S, Causon I, Floristeanu I, Chan KX, Moore CE, Diers BW, Long SP. 2020. Variation in relaxation of non-photochemical quenching in a soybean nested association mapping panel as a potential source for breeding improved photosynthesis. bioRxciv.

Cao H, Guo S, Xu Y, Jiang K, Jones AM, Chong K. 2011. Reduced expression of a gene encoding a Golgi localized monosaccharide transporter (OsGMST1) confers hypersensitivity to salt in rice (Oryza sativa). Journal of experimental botany **62**, 4595–4604.

Cavanagh AP, Slattery R, Kubien DS. 2022. Temperature induced changes in Arabidopsis Rubisco activity and isoform expression. Journal of experimental botany.

Caye K, Jumentier B, Lepeule J, François O. 2019. LFMM 2: Fast and Accurate Inference of Gene-Environment Associations in Genome-Wide Studies. Molecular biology and evolution **36**, 852–860.

Čepl J, Holá D, Stejskal J, *et al.* 2016. Genetic variability and heritability of chlorophyll a fluorescence

Accepted Manuscript

Downloaded from https://academic.oup.com/jxb/advance-article/doi/10.1093/jxb/erad239/7205185 by guest on 27 June 2023

parameters in Scots pine (Pinus sylvestris L.). Tree physiology **36**, 883–895.

Chen YE, Cui JM, Li GX, Yuan M, Zhang ZW, Yuan S, Zhang HY. 2016. Effect of salicylic acid on the antioxidant system and photosystem II in wheat seedlings. Biologia plantarum **60**, 139–147.

Chen Y-E, Mao H-T, Wu N, Din AMU, Khan A, Zhang H-Y, Yuan S. 2020. Salicylic Acid Protects Photosystem II by Alleviating Photoinhibition in Arabidopsis thaliana under High Light. International Journal of Molecular Sciences **21**, 1229.

Chen G, Zou Y, Hu J, Ding Y. 2018. Genome-wide analysis of the rice PPR gene family and their expression profiles under different stress treatments. BMC genomics **19**, 720.

Chi W, Ma J, Zhang D, Guo J, Chen F, Lu C, Zhang L. 2008. The pentratricopeptide repeat protein DELAYED GREENING1 is involved in the regulation of early chloroplast development and chloroplast gene expression in Arabidopsis. Plant physiology **147**, 573–584.

Cho M-H, Lim H, Shin DH, Jeon J-S, Bhoo SH, Park Y-I, Hahn T-R. 2011. Role of the plastidic glucose translocator in the export of starch degradation products from the chloroplasts in Arabidopsis thaliana. The New phytologist **190**, 101–112.

Coast O, Posch BC, Rognoni BG, *et al.* 2022. Wheat photosystem II heat tolerance: evidence for genotype-by-environment interactions. The Plant Journal **111**, 1368–1382.

Cowling SB, Treeintong P, Ferguson JN, Solatani H, Swarip R, Mayes S, Murchie EH. 2021. Out of Africa: characterising the natural variation in dynamic photosynthetic traits in a diverse population of African rice (Oryza glaberrima). Journal of Experimental Botany **73**, 10

Cubry P, Pidon H, Ta KN, *et al.* 2020. Genome Wide Association Study Pinpoints Key Agronomic QTLs in African Rice Oryza glaberrima. Rice **13**, 66.

Cubry P, Tranchant-Dubreuil C, Thuillet A-C, *et al.* 2018. The Rise and Fall of African Rice Cultivation Revealed by Analysis of 246 New Genomes. Current biology: CB **28**, 2274–2282.e6.

Das K, Roychoudhury A. 2014. Reactive oxygen species (ROS) and response of antioxidants as ROS-scavengers during environmental stress in plants. Frontiers in Environmental Science **2**.

Dat JF, Foyer CH, Scott IM. 1998. Changes in salicylic acid and antioxidants during induced thermotolerance in mustard seedlings. Plant physiology **118**, 1455–1461.

Dharmawardhana P, Ren L, Amarasinghe V, Monaco M, Thomason J, Ravenscroft D, McCouch S, Ware D, Jaiswal P. 2013. A genome scale metabolic network for rice and accompanying analysis of tryptophan, auxin and serotonin biosynthesis regulation under biotic stress. Rice **6**, 15.

Feeley K, Martinez-Villa J, Perez T, Duque AS, Gonzalez DT, Duque A. 2020. The Thermal Tolerances, Distributions, and Performances of Tropical Montane Tree Species. Frontiers in Forests and Global Change **3**.

Ferguson JN, McAusland L, Smith KE, Price AH, Wilson ZA, Murchie EH. 2020. Rapid temperature responses of photosystem II efficiency forecast genotypic variation in rice vegetative heat tolerance. The Plant journal: for cell and molecular biology **104**, 839–855.

Ferguson JN, Tidy AC, Murchie EH, Wilson ZA. 2021. The potential of resilient carbon dynamics for stabilizing crop reproductive development and productivity during heat stress. Plant, cell & environment **44**, 2066–2089.

Accepted Manuscript

Downloaded from https://academic.oup.com/jxb/advance-article/doi/10.1093/jxb/erad239/7205185 by guest on 27 June 2023

Ferguson JN, Jitesh T, Lawson T, Kromdijk K. 2023. Leaf excision has minimal impact on photosynthetic parameters across crop functional types. bioRxiv 2023.04. 25.548279

Flood PJ, Kruijer W, Schnabel SK, van der Schoor R, Jalink H, Snel JFH, Harbinson J, Aarts MGM. 2016. Phenomics for photosynthesis, growth and reflectance in Arabidopsis thaliana reveals circadian and long-term fluctuations in heritability. Plant methods **12**, 14.

Foyer CH, Hanke G. 2022. ROS production and signalling in chloroplasts: cornerstones and evolving concepts. The Plant Journal **111**

Frichot E, Schoville SD, Bouchard G, François O. 2013. Testing for associations between loci and environmental gradients using latent factor mixed models. Molecular biology and evolution **30**, 1687–1699.

Heo AJ, Kim SB, Ji CH, *et al.* 2021. The N-terminal cysteine is a dual sensor of oxygen and oxidative stress. Proceedings of the National Academy of Sciences of the United States of America **118**.

Herritt M, Dhanapal AP, Purcell LC, Fritschi FB. 2018. Identification of genomic loci associated with 21chlorophyll fluorescence phenotypes by genome-wide association analysis in soybean. BMC plant biology **18**, 312.

Herritt MT, Fritschi FB. 2020. Characterization of Photosynthetic Phenotypes and Chloroplast Ultrastructural Changes of Soybean (Glycine max) in Response to Elevated Air Temperatures. Frontiers in Plant Science **11**.

Holdsworth MJ, Vicente J, Sharma G, Abbas M, Zubrycka A. 2020. The plant N-degron pathways of ubiquitin-mediated proteolysis. Journal of integrative plant biology **62**, 70–89.

Hotto AM, Castandet B, Gilet L, Higdon A, Condon C, Stern DB. 2015. Arabidopsis chloroplast mini-ribonuclease III participates in rRNA maturation and intron recycling. The Plant cell **27**, 724–740.

Ishimaru T, Hirabayashi H, Sasaki K, Ye C, Kobayashi A. 2016. Breeding efforts to mitigate damage by heat stress to spikelet sterility and grain quality. Plant Production Science **19**, 12–21.

Jagadish SVK. 2020. Heat stress during flowering in cereals - effects and adaptation strategies. The New phytologist **226**, 1567–1572.

Jagadish KSV, Kavi Kishor PB, Bahuguna RN, von Wirén N, Sreenivasulu N. 2015. Staying Alive or Going to Die During Terminal Senescence—An Enigma Surrounding Yield Stability. Frontiers in Plant Science **6**.

Jahan MS, Wang Y, Shu S, Zhong M, Chen Z, Wu J, Sun J, Guo S. 2019. Exogenous salicylic acid increases the heat tolerance in Tomato (Solanum lycopersicum L) by enhancing photosynthesis efficiency and improving antioxidant defense system through scavenging of reactive oxygen species. Scientia Horticulturae **247**, 421–429.

Janda T, Lejmel MA, Molnár AB, Majláth I, Pál M, Nguyen QT, Nguyen NT, Le VN, Szalai G. 2020. Interaction between elevated temperature and different types of Na-salicylate treatment in Brachypodium dystachion. PloS one **15**, e0227608.

Järvi S, Isojärvi J, Kangasjärvi S, Salojärvi J, Mamedov F, Suorsa M, Aro E-M. 2016. Photosystem II Repair and Plant Immunity: Lessons Learned from Arabidopsis Mutant Lacking the THYLAKOID LUMEN PROTEIN 18.3. Frontiers in plant science **7**, 405.

Accepted Manuscript

Downloaded from https://academic.oup.com/jxb/advance-article/doi/10.1093/jxb/erad239/7205185 by guest on 27 June 2023

Jing Y, Liu C, Liu B, Pei T, Zhan M, Li C, Wang D, Li P, Ma F. 2022. Overexpression of the FERONIA receptor kinase MdMRLK2 confers apple drought tolerance by regulating energy metabolism and free amino acids production. Tree physiology.

Kang HM, Zaitlen NA, Wade CM, Kirby A, Heckerman D, Daly MJ, Eskin E. 2008. Efficient control of population structure in model organism association mapping. Genetics **178**, 1709–1723.

Kaplan F, Guy CL. 2004. beta-Amylase induction and the protective role of maltose during temperature shock. Plant physiology **135**, 1674–1684.

Kaplan F, Guy CL. 2005. RNA interference of Arabidopsis beta-amylase8 prevents maltose accumulation upon cold shock and increases sensitivity of PSII photochemical efficiency to freezing stress. The Plant journal: for cell and molecular biology **44**, 730–743.

Khan S, Anwar S, Yasin Ashraf M, Khaliq B, Sun M, Hussain S, Gao Z-Q, Noor H, Alam S. 2019. Mechanisms and Adaptation Strategies to Improve Heat Tolerance in Rice. A Review. Plants **8**, 508.

Khan MIR, Iqbal N, Masood A, Per TS, Khan NA. 2013. Salicylic acid alleviates adverse effects of heat stress on photosynthesis through changes in proline production and ethylene formation. Plant signaling & behavior **8**, e26374.

Kilasi NL, Singh J, Vallejos CE, Ye C, Krishna Jagadish SV, Kusolwa P, Rathinasabapathi B. 2018. Heat Stress Tolerance in Rice (Oryza sativa L.): Identification of Quantitative Trait Loci and Candidate Genes for Seedling Growth Under Heat Stress. Frontiers in Plant Science **9**.

Lafarge T, Julia C, Baldé A, Ahmadi N, Muller B, Dingkuhn M. 2016. Rice Adaptation Strategies in Response to Heat Stress at Flowering. Climate Change and Agriculture Worldwide, 31–43.

Lee W-S, Devonshire BJ, Hammond-Kosack KE, Rudd JJ, Kanyuka K. 2015. Deregulation of Plant Cell Death Through Disruption of Chloroplast Functionality Affects Asexual Sporulation of Zymoseptoria tritici on Wheat. Molecular plant-microbe interactions: MPMI **28**, 590–604.

Lee J, Han C-T, Hur Y. 2013. Molecular characterization of the Brassica rapa auxin-repressed, superfamily genes, BrARP1 and BrDRM1. Molecular Biology Reports **40**, 197–209.

Li G, Chen T, Feng B, Peng S, Tao L, Fu G. 2021. Respiration, Rather Than Photosynthesis, Determines Rice Yield Loss Under Moderate High-Temperature Conditions. Frontiers in plant science **12**, 678653.

Lipka AE, Tian F, Wang Q, Peiffer J, Li M, Bradbury PJ, Gore MA, Buckler ES, Zhang Z. 2012. GAPIT: genome association and prediction integrated tool. Bioinformatics **28**, 2397–2399.

Lípová L, Krchnák P, Komenda J, Ilík P. 2010. Heat-induced disassembly and degradation of chlorophyll-containing protein complexes in vivo. Biochimica et biophysica acta **1797**, 63–70.

Liu W-C, Song R-F, Zheng S-Q, Li T-T, Zhang B-L, Gao X, Lu Y-T. 2022. Coordination of plant growth and abiotic stress responses by tryptophan synthase β subunit 1 through modulation of tryptophan and ABA homeostasis in Arabidopsis. Molecular plant **15**, 973–990.

Liu G, Zha Z, Cai H, *et al.* 2020. Dynamic Transcriptome Analysis of Anther Response to Heat Stress during Anthesis in Thermotolerant Rice (Oryza sativa L.). International Journal of Molecular Sciences **21**, 1155.

Lydakis-Simantiris N, Hutchison RS, Betts SD, Barry BA, Yocum CF. 1999. Manganese stabilizing protein of photosystem II is a thermostable, natively unfolded polypeptide. Biochemistry **38**, 404–

Accepted Manuscript

Downloaded from https://academic.oup.com/jxb/advance-article/doi/10.1093/jxb/erad239/7205185 by guest on 27 June 2023

414.

Maslenkova L, Peeva V, Stojnova Z, Popova L. 2009. Salicylic Acid-Induced Changes in Photosystem II Reactions in Barley Plants. Biotechnology & Biotechnological Equipment **23**, 297–300.

Maxwell K, Johnson GN. 2000. Chlorophyll fluorescence—a practical guide. Journal of Experimental Botany **51**, 659–668.

McAusland L, Atkinson JA, Lawson T, Murchie EH. 2019. High throughput procedure utilising chlorophyll fluorescence imaging to phenotype dynamic photosynthesis and photoprotection in leaves under controlled gaseous conditions. Plant methods **15**, 109.

McCormack E, Braam J. 2003. Calmodulins and related potential calcium sensors of Arabidopsis. The New phytologist **159**, 585–598.

Mi H, Muruganujan A, Huang X, Ebert D, Mills C, Guo X, Thomas PD. 2019. Protocol Update for large-scale genome and gene function analysis with the PANTHER classification system (v.14.0). Nature Protocols **14**, 703–721.

Motohashi R, Yamazaki T, Myouga F, *et al.* 2007. Chloroplast ribosome release factor 1 (AtcpRF1) is essential for chloroplast development. Plant molecular biology **64**, 481–497.

Muggeo VMR. 2017. Interval estimation for the breakpoint in segmented regression: a smoothed score-based approach. Australian & New Zealand Journal of Statistics **59**, 311–322.

Mühlenbeck H, Bender KW, Zipfel C. 2021. Importance of tyrosine phosphorylation for transmembrane signaling in plants. Biochemical Journal **478**, 2759–2774.

Murata N, Nishiyama Y. 2018. ATP is a driving force in the repair of photosystem II during photoinhibition. Plant, cell & environment **41**, 285–299.

Murchie EH, Lawson T. 2013. Chlorophyll fluorescence analysis: a guide to good practice and understanding some new applications. Journal of Experimental Botany **64**, 3983–3998.

Nazar R, Iqbal N, Syeed S, Khan NA. 2011. Salicylic acid alleviates decreases in photosynthesis under salt stress by enhancing nitrogen and sulfur assimilation and antioxidant metabolism differentially in two mungbean cultivars. Journal of plant physiology **168**, 807–815.

Norton GJ, Travis AJ, Douglas A, *et al.* 2018. Genome Wide Association Mapping of Grain and Straw Biomass Traits in the Rice Bengal and Assam Aus Panel (BAAP) Grown Under Alternate Wetting and Drying and Permanently Flooded Irrigation. Frontiers in plant science **9**, 1223.

Purcell S, Neale B, Todd-Brown K, *et al.* 2007. PLINK: a tool set for whole-genome association and population-based linkage analyses. American journal of human genetics **81**, 559–575.

Qu Y, Sakoda K, Fukayama H, Kondo E, Suzuki Y, Makino A, Terashima I, Yamori W. 2021. Overexpression of both Rubisco and Rubisco activase rescues rice photosynthesis and biomass under heat stress. Plant, cell & environment **44**, 2308–2320.

Rosa M, Abraham-Juárez MJ, Lewis MW, Fonseca JP, Tian W, Ramirez V, Luan S, Pauly M, Hake S. 2017. The Maize MID-COMPLEMENTING ACTIVITY Homolog CELL NUMBER REGULATOR13/NARROW ODD DWARF Coordinates Organ Growth and Tissue Patterning. The Plant cell **29**, 474–490.

Ruiz-Vera UM, Siebers MH, Jaiswal D, Ort DR, Bernacchi CJ. 2018. Canopy warming accelerates

Accepted Manuscript

Downloaded from https://academic.oup.com/jxb/advance-article/doi/10.1093/jxb/erad239/7205185 by guest on 27 June 2023

development in soybean and maize, offsetting the delay in soybean reproductive development by elevated CO concentrations. Plant, cell & environment **41**, 2806–2820.

Salvucci ME, Crafts-Brandner SJ. 2004. Inhibition of photosynthesis by heat stress: the activation state of Rubisco as a limiting factor in photosynthesis. Physiologia plantarum **120**, 179–186.

Sathe AP, Su X, Chen Z, Chen T, Wei X, Tang S, Zhang X-B, Wu J-L. 2019. Identification and characterization of a spotted-leaf mutant spl40 with enhanced bacterial blight resistance in rice. Rice **12**, 68.

Satou M, Enoki H, Oikawa A, *et al.* 2014. Integrated analysis of transcriptome and metabolome of Arabidopsis albino or pale green mutants with disrupted nuclear-encoded chloroplast proteins. Plant molecular biology **85**, 411–428.

Sharkey TD. 2005. Effects of moderate heat stress on photosynthesis: importance of thylakoid reactions, rubisco deactivation, reactive oxygen species, and thermotolerance provided by isoprene. Plant, Cell and Environment **28**, 269–277.

Sharma E, Borah P, Kaur A, Bhatnagar A, Mohapatra T, Kapoor S, Khurana JP. 2021. A comprehensive transcriptome analysis of contrasting rice cultivars highlights the role of auxin and ABA responsive genes in heat stress response. Genomics **113**, 1247–1261.

Sharma DK, Torp AM, Rosenqvist E, Ottosen C-O, Andersen SB. 2017. QTLs and Potential Candidate Genes for Heat Stress Tolerance Identified from the Mapping Populations Specifically Segregating for Fv/Fm in Wheat. Frontiers in plant science **8**, 1668.

Shen J-R. 2015. The Structure of Photosystem II and the Mechanism of Water Oxidation in Photosynthesis. Annual Review of Plant Biology **66**, 23–48.

Shin JH, Blay S, McNeney B, Graham J. 2006. LDheatmap: An R Function for Graphical Display of Pairwise Linkage Disequilibria Between Single Nucleotide Polymorphisms. Journal of statistical software **16**.

Shin SY, Park J-S, Park H-B, Moon K-B, Kim H-S, Jeon J-H, Cho HS, Lee H-J. 2021. FERONIA Confers Resistance to Photooxidative Stress in Arabidopsis. Frontiers in plant science **12**, 714938.

Song P, Wang J, Guo X, Yang W, Zhao C. 2021. High-throughput phenotyping: Breaking through the bottleneck in future crop breeding. The Crop Journal **9**, 633–645.

Sun T, Hasegawa T, Liu B, Tang L, Liu L, Cao W, Zhu Y. 2021. Current rice models underestimate yield losses from short-term heat stresses. Global change biology **27**, 402–416.

Sun J, Tian Y, Lian Q, Liu J-X. 2020. Mutation of DELAYED GREENING1 impairs chloroplast RNA editing at elevated ambient temperature in Arabidopsis. Journal of genetics and genomics = Yi chuan xue bao **47**, 201–212.

Sun Q, Zhao Y, Zhang Y, Chen S, Ying Q, Lv Z, Che X, Wang D. 2022. Heat stress may cause a significant reduction of rice yield in China under future climate scenarios. Science of The Total Environment **818**, 151746.

Theis J, Schroda M. 2016. Revisiting the photosystem II repair cycle. Plant signaling & behavior **11**, e1218587.

Thompson LK, Blaylock R, Sturtevant JM, Brudvig GW. 1989. Molecular basis of the heat

Accepted Manuscript

Downloaded from https://academic.oup.com/jxb/advance-article/doi/10.1093/jxb/erad239/7205185 by guest on 27 June 2023

denaturation of photosystem II. Biochemistry **28**, 6686–6695.

Tiwari A, Singh P, Riyazat Khadim S, Singh AK, Singh U, Singh P, Asthana RK. 2019. Role of Ca as protectant under heat stress by regulation of photosynthesis and membrane saturation in Anabaena PCC 7120. Protoplasma **256**, 681–691.

Turner SD. 2018. qqman: an R package for visualizing GWAS results using Q-Q and manhattan plots. The Journal of Open Source Software **3(25)**.

Wang Y, Cui X, Yang B, *et al.* 2020*a*. WRKY55 transcription factor positively regulates leaf senescence and the defense response by modulating the transcription of genes implicated in the biosynthesis of reactive oxygen species and salicylic acid in. Development **147**.

Wang W, Mauleon R, Hu Z, *et al.* 2018. Genomic variation in 3,010 diverse accessions of Asian cultivated rice. Nature **557**, 43–49.

Wang L, Yang T, Wang B, *et al.* 2020*b*. RALF1-FERONIA complex affects splicing dynamics to modulate stress responses and growth in plants. Science advances **6**, eaaz1622.

Wang Q, Yang S, Wan S, Li X. 2019. The Significance of Calcium in Photosynthesis. International journal of molecular sciences **20**.

Wickham H. 2007. Reshaping Data with the**reshape**Package. Journal of Statistical Software **21**.

Wickham H. 2009. *ggplot2: Elegant Graphics for Data Analysis*. Springer Science & Business Media.

Wickham H. 2011. The Split-Apply-Combine Strategy for Data Analysis. Journal of Statistical Software **40**.

Xu H, Liu G, Liu G, Yan B, Duan W, Wang L, Li S. 2014. Comparison of investigation methods of heat injury in grapevine (Vitis) and assessment to heat tolerance in different cultivars and species. BMC plant biology **14**, 156.

Xu J, Misra G, Sreenivasulu N, Henry A. 2021. What happens at night? Physiological mechanisms related to maintaining grain yield under high night temperature in rice. Plant, cell & environment **44**, 2245–2261.

Yamamoto Y. 2016. Quality Control of Photosystem II: The Mechanisms for Avoidance and Tolerance of Light and Heat Stresses are Closely Linked to Membrane Fluidity of the Thylakoids. Frontiers in plant science **7**, 1136.

Yang W, Feng H, Zhang X, Zhang J, Doonan JH, Batchelor WD, Xiong L, Yan J. 2020. Crop Phenomics and High-Throughput Phenotyping: Past Decades, Current Challenges, and Future Perspectives. Molecular plant **13**, 187–214.

Yan Q, Huang Q, Chen J, Li J, Liu Z, Yang Y, Li X, Wang J. 2017. SYTA has positive effects on the heat resistance of Arabidopsis. Plant Growth Regulation **81**, 467–476.

Yoshioka-Nishimura M. 2018. Quality Control of Photosystem II Role of Structural Changes of Thylakoid Membranes and FtsH Proteases in High Light Tolerance and Recovery from Photoinhibition. Handbook of Photosynthesis, 223–228.

Yoshioka M, Yamamoto Y. 2011. Quality control of Photosystem II: where and how does the degradation of the D1 protein by FtsH proteases start under light stress?--Facts and hypotheses.

Accepted Manuscript

Downloaded from https://academic.oup.com/jxb/advance-article/doi/10.1093/jxb/erad239/7205185 by guest on 27 June 2023

Journal of photochemistry and photobiology. B, Biology **104**, 229–235.

Zhang R, Sharkey TD. 2009. Photosynthetic electron transport and proton flux under moderate heat stress. Photosynthesis research **100**, 29–43.

Zheng H, Xu Y, Ji D, Xu K, Chen C, Wang W, Xie C. 2022. Calcium-Calmodulin-Involved Heat Shock Response of Neoporphyra haitanensis. Frontiers in Marine Science **9**.

Zhen F, Zhou J, Mahmood A, Wang W, Chang X, Liu B, Liu L, Cao W, Zhu Y, Tang L. 2020. Quantifying the effects of short-term heat stress at booting stage on nonstructural carbohydrates remobilization in rice. The Crop Journal **8**, 194–212.

Accepted Manuscript

Downloaded from https://academic.oup.com/jxb/advance-article/doi/10.1093/jxb/erad239/7205185 by guest on 27 June 2023

Figure Legends

Figure 1. Flow diagram demonstrating steps of data acquisition, data processing, and data analysis leading to the identification of candidate genes

Figure 2. Example of segmented models fitted to two distinct *Oryza sativa* accessions. The orange solid line is the mean predicted model fit from four biological repeats, where the shaded area represents the standard error of the mean. Mean T_{crit} and T_{50} are indicated with blue and green dashed lines respectively with associated standard errors. (A) Accession: IRGC_28958 (*Oryza sativa*). (B) Accession: IRGC_28994 (*Oryza sativa*)

Figure 3. Natural variation for all parameters modelled from the segmented relationship between F_v/F_m and temperature. (A-B) m_1 for *O. glaberrima* and *O. sativa* respectively. (C-D) m_2 for *O. glaberrima* and *O. sativa* respectively. (E-F) T_{crit} for *O. glaberrima* and *O. sativa* respectively. (G-H) T_{50} for *O. glaberrima* and *O. sativa* respectively.

Figure 4. Manhattan plots for genome wide association of PHT traits within the two rice populations. (A) Tcrit association with *O. glaberrima* (Og) SNPs according to FarmCPU GWAS model; (B) T50-Og association according to LFMM model; (C) Tcrit association with *O. sativa* (Os) according to EMMA model; (D) T50-Os association according to EMMA model. Solid red line indicative of suggestive SNP significance threshold based upon polygenicity assessment of QQ plots. SNPs within the identified QTLs are highlighted in green to show distinct distribution across traits and populations.

Figure 5. Precise mapping of 1Mb region (26.3- 27.3Mb) on Chromosome 11. Zoomed Manhattan plots showing SNP associations with Tcrit and T50 in the *O. sativa* population are plotted against a Linkage Disequilibrium (LD) heatmap, with blue asterisks highlighting significant SNPs (p<0.0001). All genes within the region are further plotted, with dotted lines highlighting the positions of select PHT candidate genes (Table 3) within LD (r2>0.3) of significant SNPs.

Figure 6. Gene ontology (GO) enrichment analyses. (A) Significantly enriched biological processes terms within the identified gene list. (B) Significantly enriched molecular functions terms within the identified gene list.

Accepted Manuscript

Downloaded from https://academic.oup.com/jxb/advance-article/doi/10.1093/jxb/erad239/7205185 by guest on 27 June 2023

Tables

Table 1. The population mean, broad sense heritability (H^2), and goodness of fit of the linear mixed model (R^2) for each trait measured on each species

Trait (Species)	Population Mean	H^2	R^2
T_{50} (*O. glaberrima*)	46.847	0.53	0.76
T_{crit} (*O. glaberrima*)	44.709	0.61	0.83
m_1 (*O. glaberrima*)	-0.005	0.27	0.42
m_2 (*O. glaberrima*)	-0.151	0.09	0.18
T_{50} (*O. sativa*)	48.763	0.61	0.74
T_{crit} (*O. sativa*)	46.415	0.65	0.72
m_1 (*O. sativa*)	-0.005	0.48	0.49
m_2 (*O. sativa*)	-0.132	0.53	0.52

Accepted Manuscript

Downloaded from https://academic.oup.com/jxb/advance-article/doi/10.1093/jxb/erad239/7205185 by guest on 27 June 2023

Table 2. Location of putative QTLs identified from GWAS of T50 and Tcrit traits within the Bengal Assam Aus sub-population of *Oryza sativa* (BAAP) and sub-population of *Oryza glaberrima* (Glab). Maximum number of significant SNPs within the QTL is reported according to the best (a) and 2nd best (b) fit GWAS model.

	QTL location			Number of significant SNPs			
QTL-ID	**Chr**	**Range**	**Peak (Mb)**	**T50-BAAP**	**Tcrit-BAAP**	**T50- Glab**	**Tcrit-Glab**
Os-T50-2a	2	10.06-10.14	10.059	2 [ab]	1 [a]		
Os-Tcrit-2	2	14.57-14.71	14.568		3 [a]		
Os-T50-2b	2	24.29-24.38	24.382	2 [a]	1 [b]		
Og-Tcrit-3	3	1.61-1.61	1.61				2 [a]
Os-Tcrit-3	3	17.89-17.89	17.894		3 [a]		
Os-Tcrit-5	5	14.45-14.45	14.452		2 [b]		
Og-Tcrit-7	7	22.24-22.26	22.256				3 [a]
Og-T50-8	8	1.71-1.78	1.757			20 [a]	
Os-T50-9	9	8.76-8.76	8.757	2 [a]			
Os-T50-10	10	6.25-6.25	6.255	2 [b]			

Accepted Manuscript

Downloaded from https://academic.oup.com/jxb/advance-article/doi/10.1093/jxb/erad239/7205185 by guest on 27 June 2023

Og-Tcrit-11	11	4.96-4.97	4.964				2^{a}
Os-Tcrit-11a	11	16.88-16.89	16.88	1^{b}	2^{ab}		
Os-T50-11a	11	23.25-23.51	23.25	3^{a}	1^{a}		
Os-T50-11b	11	26.40-26.48	26.456	12^{a}			
Os-Tcrit-11b	11	26.81-27.25	26.978		40^{b}		

Accepted Manuscript

Downloaded from https://academic.oup.com/jxb/advance-article/doi/10.1093/jxb/erad239/7205185 by guest on 27 June 2023

Table 3. Candidate genes underlying QTLs from BAAP population with relevant functions, according to literature analysis, Differentially Expressed Genes (DEG) showing a more than 2-fold change in response to 37/42C heat in IR64/ Annapurna seedlings according to RNASeq (Sharma et al., 2021) and chloroplast (Chl.) localisation according to Gene Ontology (GO) analysis of cellular compartment.

Loci (&QTL)	Name	Description	Function	DEG	Chl.
Os02g0274900 (Os-T50-2a)	GMST1	*golgi localized monosaccharide transporter 1*	Photosynthesis & carbon partitioning (Arabidopsis)[1]	-	*
Os02g0275200 (Os-T50-2a)	FUT1	*galactoside 2-alpha-L-fucosyltransferase*	-	DOWN	-
Os02g0276200 (Os-T50-2a)	-	*probable inactive nicotinamidase At3g16190*	-	UP	-
Os02g0448400 (Os-Tcrit-2)	SYN2	*synaptotagmin-2*	Heat stress (Arabidopsis)[2]	-	-
Os02g0448600 (Os-Tcrit-2)	-	*pentatricopeptide (PPR) repeat-containing protein-like At4g22758*	-	-	*
Os05g0311500 (Os-Tcrit-5)	LOR8	*protein LURP-one-related 8*	-	DOWN	-

Accepted Manuscript

Downloaded from https://academic.oup.com/jxb/advance-article/doi/10.1093/jxb/erad239/7205185 by guest on 27 June 2023

Os05g0311801 (Os-Tcrit-5)	IPT3	*adenylate isopentenyltransferase 3*	-	-	*
Os05g0312000 (Os-Tcrit-5)	SPL40	*mediator of RNA polymerase II transcription subunit 33A*	Photosynthesis & disease resistance (Rice)[3]	UP	-
Os05g0312600 (Os-Tcrit-5)	CML21	*calmodulin-like protein 21*	Abiotic stress response (Grapevine)[4]	-	*
Os05g0314700 (Os-Tcrit-5)	-	*uncharacterized protein*	-	UP	-
Os05g0315100 (Os-Tcrit-5)	OsDG1	*delayed greening 1*	Chloroplast development (Arabidopsis[5]) & stress response (Rice[6])	UP	*
Os05g0316100 (Os-Tcrit-5)	-	*putative zinc transporter At3g08650*	-	UP	-
Os05g0316200 (Os-Tcrit-5)	-	*protein SSUH2 homolog*	-	UP	-
Os05g0317200 (Os-Tcrit-5)	LACS8	*long chain acyl-CoA synthetase 8*	-	-	*

Accepted Manuscript

Downloaded from https://academic.oup.com/jxb/advance-article/doi/10.1093/jxb/erad239/7205185 by guest on 27 June 2023

Os05g0318300 (Os-Tcrit-5)	RNC3	*chloroplast mini-ribonuclease III At1g55140*	Chlorophyll accumulation (Arabidopsis)[7]	DOWN	*
Os05g0317700 (Os-Tcrit-5)	OsANX2	*receptor-like protein kinase FERONIA*	-	DOWN	-
Os05g0318600 (Os-Tcrit-5)	-	*LOW QUALITY PROTEIN: receptor-like protein kinase FERONIA*	-	DOWN	-
Os05g0320800 (Os-Tcrit-5)	-	*uncharacterized protein*	-	DOWN	-
Os05g0321900 (Os-Tcrit-5)	WRKY55	*WRKY transcription factor 55*	Leaf senescence & defence (Arabidopsis)[8]	-	-
Os11g0484500 (Os-Tcrit-11a)	PGD2	*6-phosphogluconate dehydrogenase, decarboxylating 2*	-	-	*
Os11g0603200 (Os-T50-11a)	ABCF5	*ABC transporter F family member 5*	-	DOWN	*
Os11g0657100 (Os-T50-11b)	APG3	*albino or pale green 3*	Chloroplast development (Arabidopsis)[9]	-	*
Os11g0659200 (Os-T50-11b)	FLZ15	*FCS-Like zinc finger 15*	-	UP	*

Accepted Manuscript

Downloaded from https://academic.oup.com/jxb/advance-article/doi/10.1093/jxb/erad239/7205185 by guest on 27 June 2023

Os11g0659500 (Os-T50-11b)	FATB	*palmitoyl-acyl carrier protein thioesterase*	-	-	*
Os11g0669100 (Os-Tcrit-11b)	CBP60B	*calmodulin-binding protein 60 B*	-	DOWN	-
Os11g0670900 (Os-Tcrit-11b)	-	*uncharacterized protein*	-	UP	-
Os11g0671000 (Os-Tcrit-11b)	DRM1	*dormancy-associated protein 1*	Heat shock (Brassica)[10]	-	-
Os11g0672300 (Os-Tcrit-11b)	CNR13	*cell number regulator 13*	Stomatal density (Maize)[11]	UP	-
Os11g0673100 (Os-Tcrit-11b)	TMEM205	*transmembrane protein 205*	-	UP	-
Os11g0678000 (Os-Tcrit-11b)	SIS8	*probable serine/threonine-protein kinase, sugar insensitive 8*	-	DOWN	-

1. Cho *et al.*, (2011); 2. Yan *et al.*, (2017); 3. Sathe *et al.*, (2019); 4. Aleynova *et al.*, (2020); 5. Chi *et al.*, (2008); 6. Chen *et al.*, (2018) 7. Hotto *et al.*, (2015); 8. Wang *et al.*, (2020*a*); 9. Satou *et al.*, (2014); 10. Lee *et al.*, (2013); 11. Rosa *et al.*, (2017)

Accepted Manuscript

Downloaded from https://academic.oup.com/jxb/advance-article/doi/10.1093/jxb/erad239/7205185 by guest on 27 June 2023

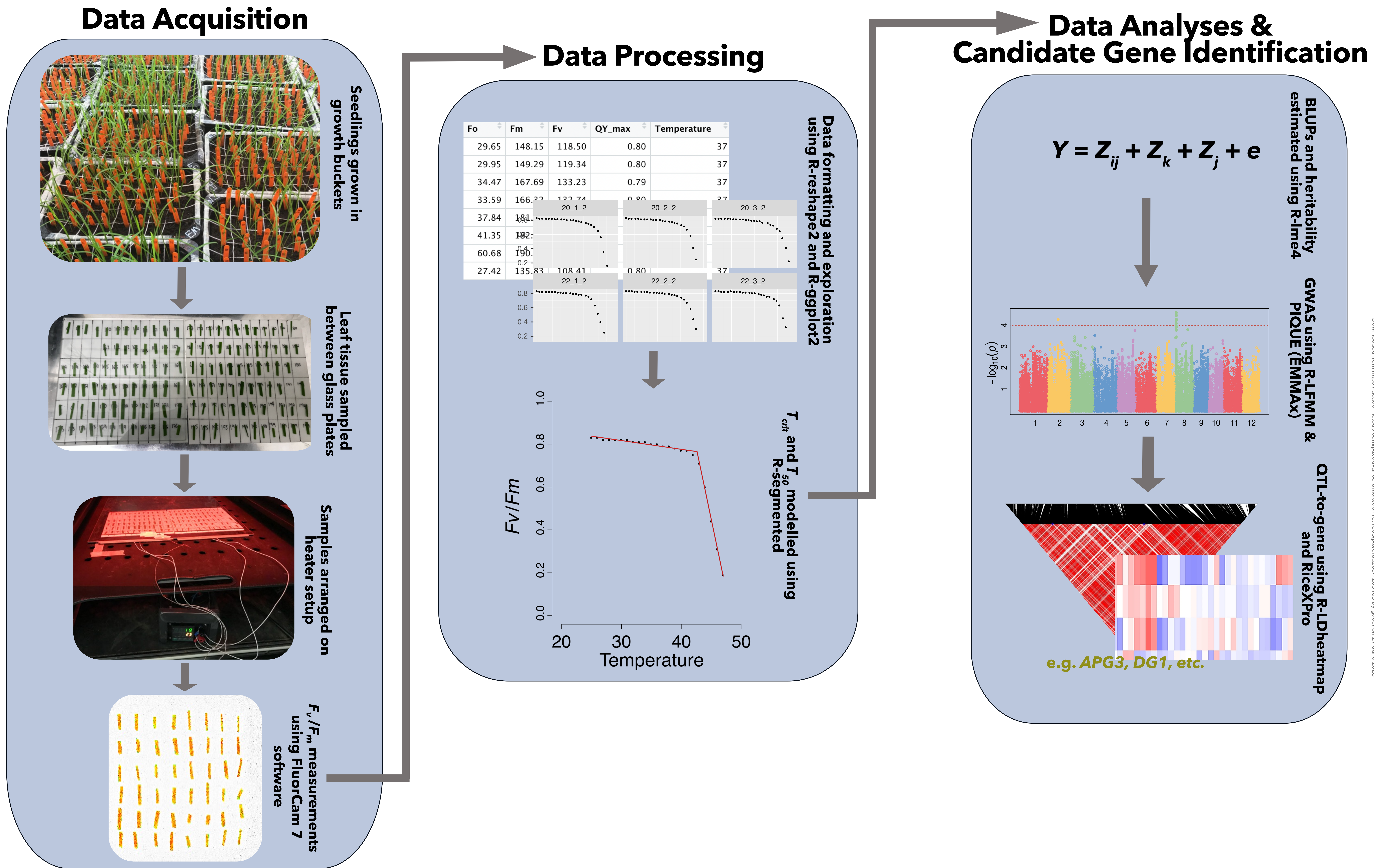

Figure 1. Flow diagram demonstrating steps of data acquisition, data processing, and data analysis leading to the identification of candidate genes

Downloaded from https://academic.oup.com/jxb/advance-article/doi/10.1093/jxb/erad239/7205185 by guest on 27 June 2023

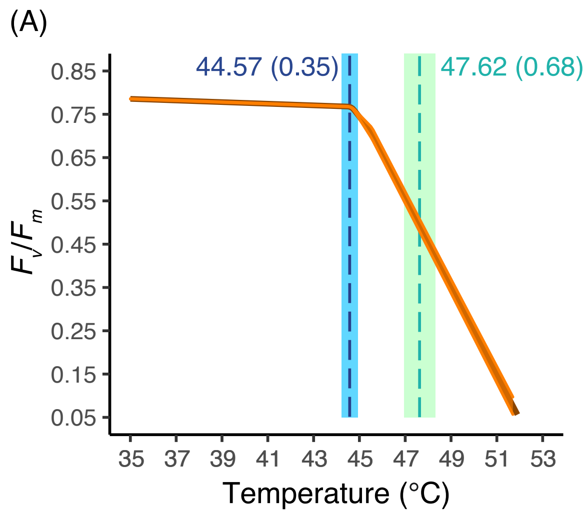

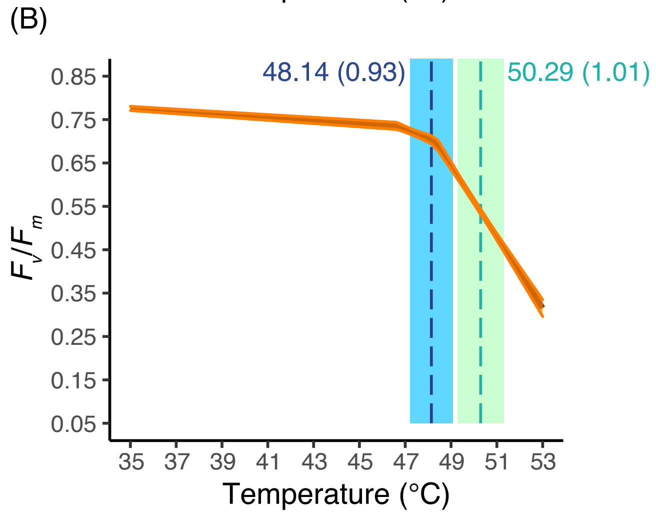

Downloaded from https://academic.oup.com/jxb/advance-article/doi/10.1093/jxb/erad239/7205185 by guest on 27 June 2023

Figure 2. Example of segmented models fitted to distinct Oryza sativa accessions. The orange solid line is the mean predicted model fit from four biological repeats, where the shaded area represents the standard error of the mean. Mean T_{crit} and T_{50} are indicated with blue and green dashed lines respectively with associated standard errors. (a) Accession: IRGC_28958(Oryza sativa). (b) Accession: IRGC_28994(Oryza sativa)

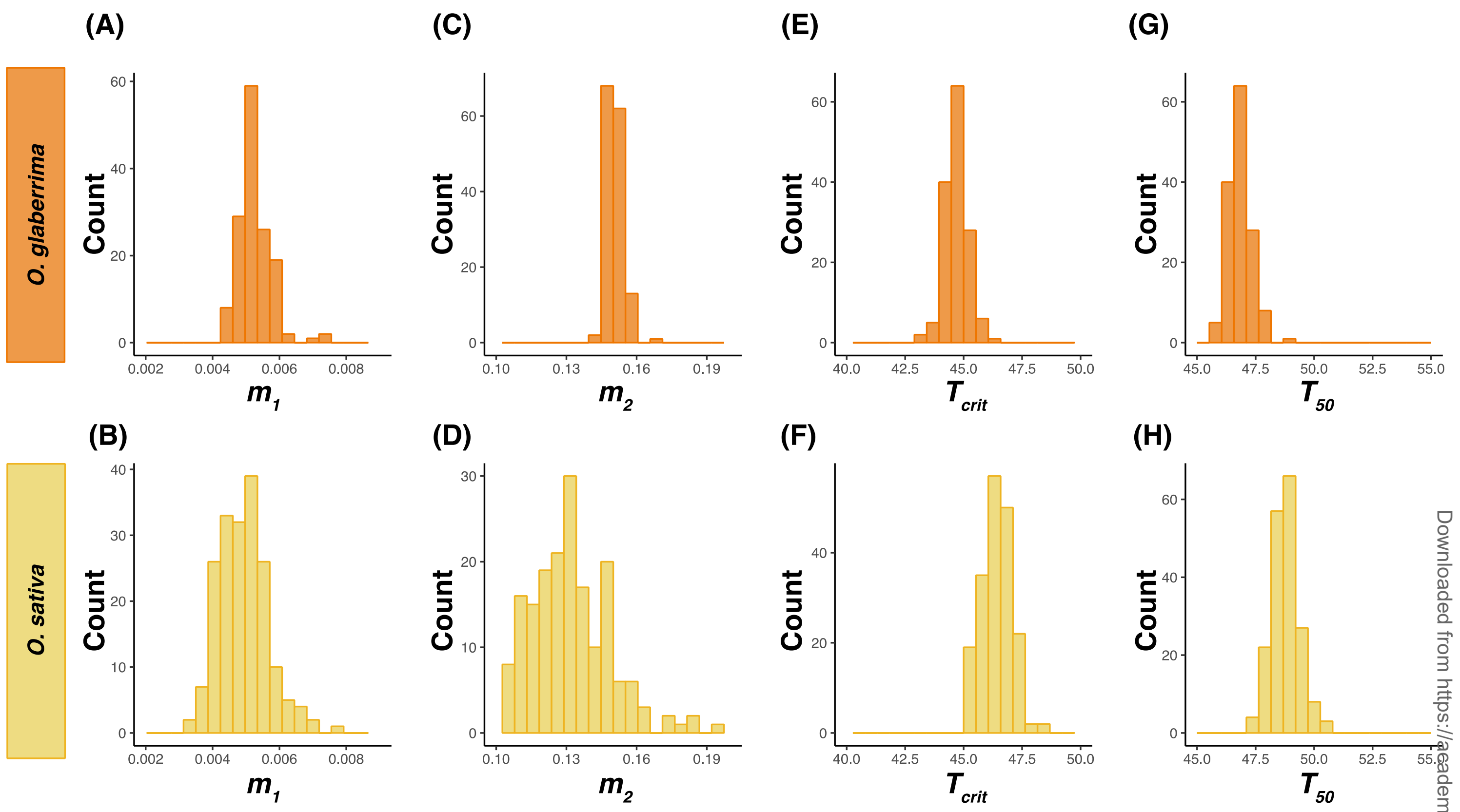

Figure 3. Natural variation for all parameters modelled from the segmented relationship between Fv/Fm and temperature.

Downloaded from https://academic.oup.com/jxb/advance-article/doi/10.1093/jxb/erad239/7205185 by guest on 27 June 2023

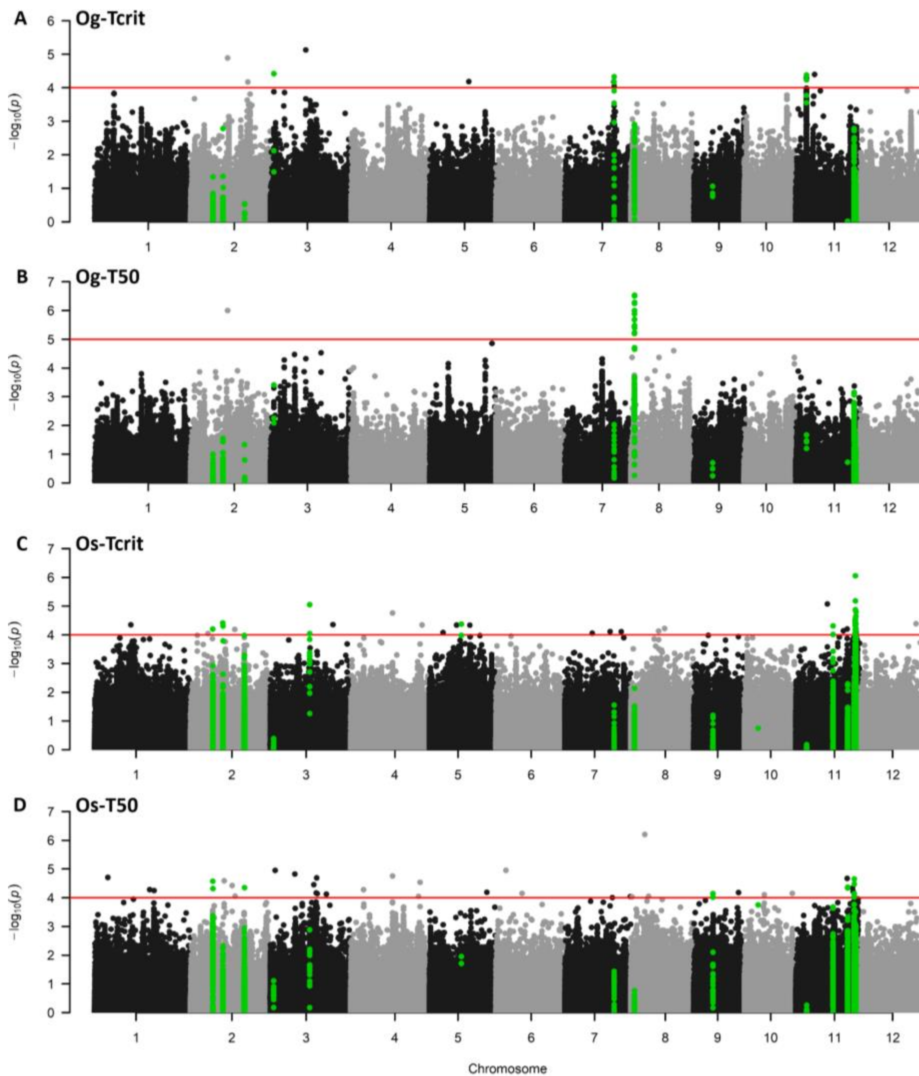

Figure 4. Manhattan plots for genome wide association of PHT traits within the two rice populations. A) Tcrit association with *O. glaberrima* (Og) SNPs according to FarmCPU GWAS model; B) T50-Og association according to LFMM model; C) Tcrit association with *O. sativa* (Os) according to EMMA model; D) T50-Os association according to EMMA model. Solid red line indicative of suggestive SNP significance threshold based upon polygenicity assessment of QQ plots. SNPs within the identified QTLs are highlighted in green to show distinct distribution across traits and populations.

Downloaded from https://academic.oup.com/jxb/advance-article/doi/10.1093/jxb/erad239/7205185 by guest on 27 June 2023

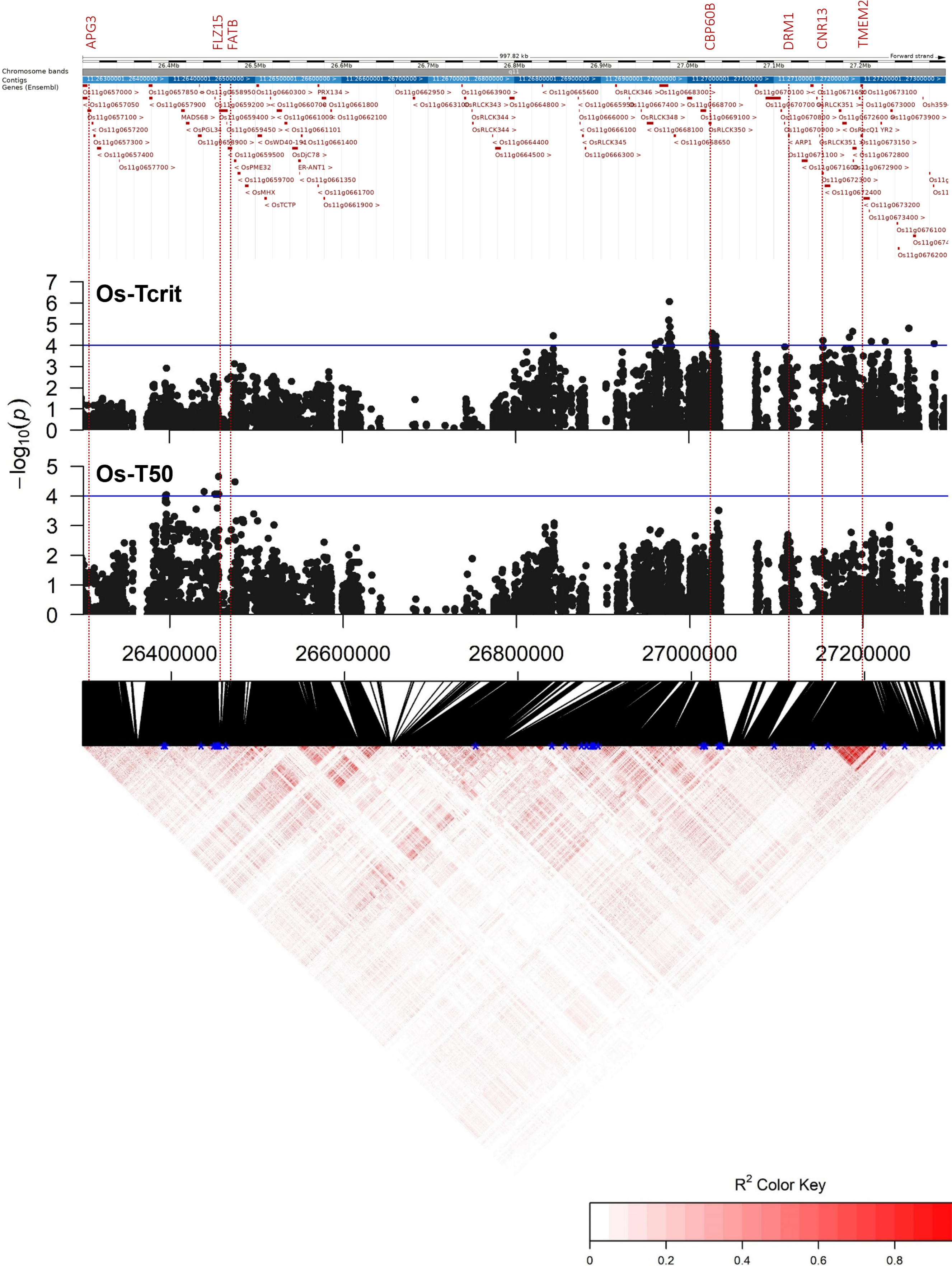

Figure 5.Precise mapping of 1Mb region (26.3- 27.3Mb) on Chromosome 11. Zoomed Manhattan plots showing SNP associations with Tcrit and T50 in the O. sativa population are plotted against a Linkage Disequilibrium (LD) heatmap, with blue asterisks highlighting significant SNPs (p<0.0001). All genes within the region are further plotted, with dotted lines highlighting the positions of select PHT candidate genes (Table 3) within LD (r2>0.3) of significant SNPs.

Downloaded from https://academic.oup.com/jxb/advance-article/doi/10.1093/jxb/erad239/7205185 by guest on 27 June 2023

Figure 6. Gene ontology (GO) enrichment analyses. (a) Significantly enriched biological processes terms within the identified gene list. (b) Significantly enriched molecular functions terms within the identified gene list.

Downloaded from https://academic.oup.com/jxb/advance-article/doi/10.1093/jxb/erad239/7205185 by guest on 27 June 2023